

UC Irvine

UC Irvine Previously Published Works

Title

DNA G-Quadruplex Is a Transcriptional Control Device That Regulates Memory.

Permalink

<https://escholarship.org/uc/item/1h67012c>

Journal

The Journal of Neuroscience, 44(15)

Authors

Marshall, Paul

Davies, Joshua

Zhao, Qiongyi

et al.

Publication Date




2024-04-10

DOI

10.1523/JNEUROSCI.0093-23.2024

Peer reviewed

DNA G-Quadruplex Is a Transcriptional Control Device That Regulates Memory

Paul R. Marshall,^{1,2} Joshua Davies,¹  Qiongyi Zhao,¹  Wei-Siang Liao,¹ Yujin Lee,¹ Dean Basic,¹ Ambika Periyakarupiah,¹ Esmi L. Zajaczkowski,¹ Laura J. Leighton,¹ Sachithrani U. Madugalle,¹ Mason Musgrove,¹ Marcin Kielar,¹ Arie Maeve Brueckner,¹  Hao Gong,¹ Haobin Ren,¹ Alexander Walsh,¹  Lech Kaczmarczyk,³ Walker S. Jackson,³ Alon Chen,⁴ Robert C. Spitale,⁵ and  Timothy W. Bredy¹

¹Cognitive Neuroepigenetics Laboratory, The Queensland Brain Institute, University of Queensland, Brisbane, QLD 4072, Australia, ²Genome Sciences and Cancer Division & Eccles Institute of Neuroscience, John Curtin School of Medical Research, Australian National University, Canberra 2601, Australia, ³Department of Biomedical and Clinical Sciences (BKV), Division of Neurobiology (NEURO), Linköping University, Linköping 581 83, Sweden, ⁴Neurobiology of Stress Laboratory, Department Brain Sciences, Weizmann Institute of Science, Rehovot 76100, Israel, and ⁵Department of Pharmaceutical Sciences, University of California Irvine, Irvine, California 92697

The conformational state of DNA fine-tunes the transcriptional rate and abundance of RNA. Here, we report that G-quadruplex DNA (G4-DNA) accumulates in neurons, in an experience-dependent manner, and that this is required for the transient silencing and activation of genes that are critically involved in learning and memory in male C57/BL6 mice. In addition, site-specific resolution of G4-DNA by dCas9-mediated deposition of the helicase DHX36 impairs fear extinction memory. Dynamic DNA structure states therefore represent a key molecular mechanism underlying memory consolidation.

One-Sentence Summary: G4-DNA is a molecular switch that enables the temporal regulation of the gene expression underlying the formation of fear extinction memory.

Key words: DNA; gene expression; memory

Significance Statement

For decades, many scientists have considered the topic of DNA structure to be solved, with the double helix of DNA existing in one stable form. However, this is not the complete story; DNA structure has a variety of states that are functional. For example, G-quadruplex DNA (G4-DNA) is a structure that is associated with DNA damage and functional impairment. While there is abundant evidence demonstrating the involvement of G4-DNA in stalling replication or transcription, our work is the first causal evidence that G4-DNA is required for both neuronal transcription and the expression of different memory states.

Introduction

The extinction of conditioned fear is an evolutionarily conserved behavioral adaptation that is critical for survival. Like other forms of learning, long-lasting memory for fear extinction

depends on coordinated changes in gene expression, particularly in the infralimbic region of the medial prefrontal cortex (ILPFC; Martin et al., 2000; Bruel-Jungerman et al., 2007; Alberini, 2009). In recent years, we and others have shown that this process involves a tightly controlled interplay between the transcriptional machinery and epigenomic mechanisms (Campbell and Wood, 2019). DNA is significantly more persistent in cells than RNA, protein, or lipids, and the mechanisms surrounding its regulation are therefore key to understanding behavioral adaptation (Marshall and Bredy, 2016). Although DNA and histone modifications have long been associated with neuronal plasticity and memory (Vanyushin, 2006; Bredy et al., 2007; Vecsey et al., 2007; Wei et al., 2012; Gräff et al., 2014; Li et al., 2014; Lepack et al., 2020), little is known about how local changes in DNA structure impact experience-dependent gene expression. This is because the relationship between DNA structure and function has primarily been attributed to the right-handed double helix,

Received Jan. 17, 2023; revised Feb. 14, 2024; accepted Feb. 20, 2024.

Author contributions: P.R.M., E.L.Z., and T.W.B. designed research; P.R.M., J.D., Q.Z., W.-S.L., Y.L., D.B., A.P., E.L.Z., L.J.L., S.U.M., M.M., M.K., A.M.B., H.G., H.R., and A.W. performed research; P.R.M., J.D., Q.Z., W.-S.L., D.B., and A.W. analyzed data; W.-S.L., M.K., L.K., W.S.J., A.C., and R.C.S. contributed unpublished reagents/analytic tools; T.W.B. wrote the paper.

We thank Ms. Rowan Tweedale for the helpful editing of the manuscript. Australian Research Council GA142202 (T.W.B.).

P.R.M. received reagents as part of an early access program and travel costs from Nanopore to present findings. All other authors declare that they have no competing interests.

Correspondence should be addressed to Paul R. Marshall at paul.marshall@anu.edu.au or Timothy W. Bredy at t.bredy@uq.edu.au.

<https://doi.org/10.1523/JNEUROSCI.0093-23.2024>

Copyright © 2024 the authors

B-DNA, first described by Watson, Crick, and Franklin. However, DNA can adopt >20 different conformational states, several of which have been linked to transcriptional activity. In addition, the biochemical conditions that promote dynamic conformational changes in DNA, including the influx of calcium, potassium, and sodium ions, are also directly involved in driving neuronal gene expression, suggesting that dynamic changes in DNA structure may be a critically important mechanism of memory.

We recently discovered that neurons can assume a left-handed conformational state (Z-DNA) in response to neural activity, which is critical for modulating the qualitative aspects of transcription and the strength of fear-related memories (Marshall et al., 2020). However, whether other DNA structures also regulate gene expression essential for memory stability is completely unexplored. G-quadruplex DNA (G4-DNA), which accumulates when guanines fold into stable four-stranded DNA structures, is known to protect DNA during replication (Henderson et al., 1987), is involved in class-switch recombination in immune cells (Qiao et al., 2017), and dynamically regulates transcription in a variety of cell types (Kim, 2017). Like Z-DNA, G4-DNA is stabilized by ions that are highly abundant in activated neurons (Sen and Gilbert, 1990) and the folding kinetics of G4-DNA ranges from milliseconds to minutes, which overlaps temporally with the rate of transcription associated with learning. Moreover, G4-DNA helicases, such as the DEAD-Box helicase 36 (DHX36), mediate the resolution of G4-DNA structure, a process that is strongly associated with the modification of transcription (Chen et al., 2018). We therefore posited that G4-DNA is involved in the regulation of experience-dependent gene expression and memory. Here, we tested the hypothesis that the formation of G4-DNA and its resolution by DHX36 alter the rate of learning-induced transcription in the medial prefrontal cortex (mPFC) and that this process is directly related to the formation of fear-related memories.

Materials and Methods

Animals

Wild-type 9–11-week-old C57BL/6 male mice [Australian Research Council (ARC)] and Tagger mice (19; University of Queensland Biological Resources [UQBR]) were housed in four per cage, maintained on a 12 h light/dark schedule, and allowed free access to food and water. To allow for the identification of behavioral outliers, animals were transferred to pair-housed conditions and split with a plexiglass divider at least 24 h prior to training. All testing was conducted during the light phase in red light-illuminated testing rooms. All animal use and training, including the use of embryos, followed protocols approved by the Animal Ethics Committee of the University of Queensland and in accordance with the Australian Code of Practice for the Care and Use of Animals for Scientific Purposes (eighth edition, revised 2013).

Tagger mice

Breeding pairs were obtained directly from Prof. Walker Jackson (Linköping University). Upon receiving the mice, a colony was established at the Queensland Brain Institute and genotyped to confirm background. As described by Kaczmarczyk et al. (2019), the Tagger mice have a Cre-driven genetic cassette, which contains the enzyme UPRT, a nuclear localization tag, a tag for profiling of ribosome RNA, and a tag to identify Ago-bound small RNA. For this study self-deleting Cre, supplied by Prof. Alon Chen (Weizmann Institute of Science), was used to activate the transgene, and the UPRT enzyme was used in conjunction with 4-thiouracil (4TU) to metabolically label nascent RNA.

Lentiviral construct design and viral packaging

DHX36 and *DHX36* scrambled control knockdown lentiviral constructs. Lentiviral plasmids were generated by inserting either DHX36

or scrambled control (SC) shRNA using the following sequences for DHX36: GATCCCCGCCATCTAG CTACTATAAATTC AAGAGA TTTATAGTAGCTAGATGGCTTTTTC or DHX36 SC: GATCCCC AGTTCATTAGGCTAACGTATTTCAAGAGAATACGTTAGCCTAA TGAACTTTTTTC immediately downstream of the human H1 promoter in a modified FG12 vector (FG12H1, derived from the FG12 vector originally provided by David Baltimore, Caltech). The DHX36-dCas9 construct was generated by adding XhoI and MfeI restriction enzyme sites to a commercially available DHX36 cDNA (MBS1278832 MyBioSource). The cDNA was then cloned into the Syn1-dCas9 vector (Addgene 114194) and guide RNA into an mCherry vector (Addgene 114199). Lentivirus was prepared and maintained according to previously published protocols. All plasmids were verified by Sanger sequencing and primers used are reported in Extended Data Table 1-1.

Lentiviral delivery and behavioral analysis

Double cannulae (Plastics One) were implanted in the anterior posterior plane, along the midline, into the ILPFC. The injection locations were centered at +1.8 mm in the anteroposterior plane (AP) and –2.8 mm in the dorsoventral plane (DV). For the prelimbic prefrontal cortex, the injection locations were centered at +1.8 mm AP and –1.8 mm DV. Animals were then separated into single housing conditions and given at least 1 week to recover before being behaviorally trained as described below.

Mice were first fear conditioned and 24 h after fear conditioning (FC) were given two 1 μ l lentiviral injections over a 48 h period. After 1 week of incubation, the mice were either extinction trained or exposed to Context B for an equivalent period of time. In brief, this training consisted of two contexts (A and B). Both conditioning chambers (Coulbourn Instruments) had two transparent walls and two stainless steel walls with a steel grid floor (3.2 mm in diameter, 8 mm centers); however, the grid floor in Context B was covered by a flat white plastic transparent surface. Context A was also sprayed with a dilute lemon odor, and Context B was sprayed with a dilute vinegar odor to minimize context generalization. Cameras within the boxes captured movement and the results were processed automatically with a freezing measurement program (FreezeFrame). The program determined freezing by calculating the total time that the animal was immobile for >1 s, calculated across the training session. Data extraction was performed with Excel, which allowed for this score to be empirically assigned to any time window, for example, a preconditioned stimulus time point for 120 s prior to the onset of the first conditioned stimulus (CS) or a CS1 time point for 120 s where the first CS was present.

The training protocol consisted of 120 s before the FC period, followed by three pairings of a 120 s, 80 dB, and 16 kHz tone (CS) coterminating with a 1 s (120 s, intertrial interval, ITI), 0.7 mA footshock unconditioned stimulus. Mice were matched into equivalent treatment groups based on freezing during the third training CS. For extinction, mice were exposed in context and allowed to habituate to the chamber for 2 min, after which the extinction training (EXT) comprised 10, 30, or 60 nonreinforced 120 s CS presentations (5 s ITI). For the retention control (RC) animals, context exposure was performed following FC, but without presentation of the tones. For the retention tests, all mice were returned to either Context A or B and following a 2 min acclimation (used to minimize context generalization). As described above, freezing was assessed during three 120 s CS presentations (120 s ITI). Memory was inferred based on the percentage of time spent freezing during the tests. Prior to analysis, animals that did not reach the criterion of at least 30% freezing after the third CS were removed. Further, following behavioral analysis an outlier analysis was also performed using GraphPad Prism, and if animals were significant outliers relative to their group (of a minimum size of eight per cohort), they were also removed.

mPFC extraction and tissue preparation

Following behavioral training, animals were transported to a separate room where cervical dislocation was performed and followed by immediate extraction of the mPFC on ice. The tissue was then dounce homogenized in a 2 ml tissue grinder (Kimble Chase) with buffers and inhibitors related to downstream procedures.

Primary cortical neurons

Cortical tissue was isolated from embryonic day 16 embryos. Primary cortical neurons were isolated by removing the skull and meninges with fine-tipped tweezers. Cells were then added to a solution comprising Neurobasal medium (GIBCO 21103) containing 5% serum, B27 supplement (Invitrogen 17504-044), and 0.5–1% penicillin–streptomycin (Invitrogen 15140), made homogenous with gentle pipetting. The cells were then passed through a 40 μ m cell strainer (BD Falcon 352340) and plated onto six-well cell culture dishes coated with poly-L-ornithine (Sigma-Aldrich P2533) at a density of 1 million cells per well.

RNA and DNA extraction

Both cultured cells and tissue from mice were extracted and placed in PBS. Gentle pipetting was used for in vitro preparations to generate a homogenous solution. Tissue was prepared by dounce homogenization in 500 μ l of PBS, and RNA/DNA was extracted. For RNA, the TRIzol reagent was used according to the manufacturer's instructions (Invitrogen). DNA extraction was carried out using the DNeasy Blood & Tissue Kit (Qiagen) with RNase A (5 Prime), RNase H, and RNase T1 treatment (Invitrogen). Both extraction protocols were conducted according to the manufacturer's instructions. The concentration of DNA or RNA was measured by Qubit assay (Invitrogen).

RNase R treatment

RNase R (Lucigen, #RNR07250) treatment was performed on 1 μ g total RNA for 10 min at 37°C using 5U of enzyme. To improve RNase R processivity through structured regions of RNA (e.g., G-quadruplexes, rRNA), a LiCl-containing buffer [0.2 M Tris-HCl (pH 8), 1 M LiCl, 1 mM MgCl₂] was used instead of the original KCl-containing buffer [0.2 M Tris-HCl (pH 8), 1 M KCl, 1 mM MgCl₂] supplied with the enzyme.

qRT-PCR

One microgram of RNA was used for cDNA synthesis prepared using the QuantiTect Reverse Transcription Kit according to the manufacturer's protocol (Qiagen). Quantitative PCR was then performed on a RotorGene Q (Qiagen) real-time PCR cyclers with SYBR Green Master mix (Qiagen), using primers for target genes and β actin or phosphoglycerate kinase as an internal control. The threshold cycle for each sample was chosen from the linear range and converted to a starting quantity by interpolation from a standard curve run on the same plate for each set of primers. All mRNA levels were normalized for each well relative to the internal control using the $\Delta\Delta$ CT method, and each PCR reaction was run in duplicate for each sample and repeated at least twice. For experiments using RNase R treatment, the 2- Δ CT method was used to normalize each treated sample with its corresponding input (i.e., RNase R-).

Fluorescence-activated cell sorting (FACS)

The procedure for sorting activated neurons for cDNA preparation and ChIP-seq was modified from a previously published protocol (Li et al., 2019). Briefly, following sample preparation for FACS, the identified population of neurons using NeuN, as indicated by their high intensity in the 488 nm channel, was further split into two populations, which had an intensity in the 647 nm activity-regulated cytoskeleton (Arc) channel above the upper part of the non-NeuN population (high Arc) or below it (low Arc; Fig. 1B). A total of 250,000 cells from each sample were then taken, and four biological replicates were pooled to make one for further processing to reach at least the 1 million cells required for reliable chromatin immunoprecipitation (IP).

Chromatin IP (ChIP)

Standard ChIP was performed following modification of the Invitrogen ChIP kit protocol. Lysate from cells or tissue was fixed in 1% formaldehyde, and cross-linked cell lysates were sheared by Covaris in 1% SDS lysis buffer to generate chromatin fragments with an average length of 300 bp. For samples not subjected to sequencing, 1 million yeast (kindly provided by Prof. Michael Kobor, University of British Columbia) per sample were spiked in prior to fixation to enhance antibody-target interactions when the cell count was low (O'Neill et al., 2006). Following shearing, the chromatin was first centrifuged at 21,000 \times g for 15 min followed by the

addition of the blocking buffer and RNase A. The samples were then immunoprecipitated following a previously published protocol for G4 ChIP-seq (Hänsel-Hertsch et al., 2018), using the G4-DNA antibody (MABE917 Sigma-Aldrich) and anti-FLAG M2 beads (M8823-1ML Sigma-Aldrich).

Other ChIP experiments were carried out as described above with anti-RNA polymerase II CTD repeat YSPTSPS antibody (ab817), anti-DHX36 antibody (ab223564), or normal rabbit IgG (Santa Cruz Biotechnology), overnight at 4°C. For these experiments, ChIP dilution buffer [1% SDS, 0.01% Triton X-100, 1.2 mM EDTA, 17 mM Tris-HCl (pH 8), 165 mM NaCl] was used postshearing as it is optimized for protein G binding and the subsequent proteinase K step. Protein–DNA–antibody complexes were then precipitated with Dynabeads Protein G (Thermo Fisher Scientific 10003D) for 1 h at 4°C, followed by three washes in low salt buffer [1% SDS, 0.01% Triton X-100, 2 mM EDTA, 20 mM Tris-HCl (pH 8.0), 150 mM NaCl] and three washes in high salt buffer [1% SDS, 0.01% Triton X-100, 2 mM EDTA, 20 mM Tris-HCl (pH 8.0), 500 mM NaCl] for protein G beads, followed by resuspension in ChIP dilution buffer [1% SDS, 0.01% Triton X-100, 1.2 mM EDTA, 17 mM Tris-HCl (pH 8), 165 mM NaCl]. Precipitated protein–DNA complexes were eluted from the antibody with 1% SDS and 0.1 M NaHCO₃ and incubated for 4 h at 65°C in proteinase K. Following proteinase K digestion, phenol-chloroform extraction, and ethanol precipitation, the samples were subjected to qPCR using primers specific for 200 bp segments corresponding to the target regions (Extended Data Table 1-1). For FAIRE-seq experiments, the lysate was split into two equal volumes with half being treated with the standard protocol as described above. The other half followed the same protocol except that during the proteinase K step, no heat was applied and no proteinase K was added.

G4-seq

For G4-seq experiments, the protocol of Hänsel-Hertsch et al. (2018) was followed with the following modifications. Briefly, samples were incubated in a blocking buffer, treated with RNase A to remove RNA, and enriched with the G4 antibody. In the case of G4 experiments performed following the enrichment of neurons based on NeuN expression or activity, by Arc tagging, the enrichment was carried out by first centrifugation of the collected cells at 21,000 \times g for 15 min followed by the addition of the sonication buffer. Samples were spun postshearing followed by the addition of blocking buffer, RNaseA, and enrichment by G4-specific antibody. The rest of the protocol was the same as described above until elution. Following the elution of the DNA, the samples were subjected to three different library preparation types. Sequencing performed on both FACS and non-FACS sorted samples was prepared with the DNA HyperPrep Kit (KAPA) and sequenced on a HiSeq 2000 according to the manufacturer's recommendations. For sequencing run on the Nanopore, which consisted of FACS sorted samples, the eluted DNA was first prepared with the KAPA HyperPrep Kit, followed by native barcoding (EXP-NBD196) and a ligation sequencing kit (SQK-LSK109) from Oxford Nanopore according to the manufacturer's recommendations. Demultiplexing of samples was performed either with the KAPA adapters alone or the KAPA adapters followed by the adapters from the Nanopore native barcoding. All other bioinformatics for peak calling were performed as described below.

FAIRE (formaldehyde-assisted isolation of regulatory elements)-qPCR

In order to confirm whether G4 enrichment was occurring in chromatin-rich or chromatin-depleted regions, we performed FAIRE-qPCR. This consisted of standard G4 immunoprecipitation (G4-IP) as described above, followed by the removal of the reverse crosslinking step prior to phenol-chloroform enrichment. Standard qPCR was then performed comparing the same sample to its input and reverse cross-linked counterpart.

4TU sequencing (4-TU-seq)

The protocol was performed as described by Kaczmarczyk et al. (2019). Briefly, as described previously, animals were cannulated, and following recovery self-deleting, Cre was infused to activate the Tagger cassette. On the day of training, 1 M of 4-TU (Sigma-Aldrich) in DMSO was diluted

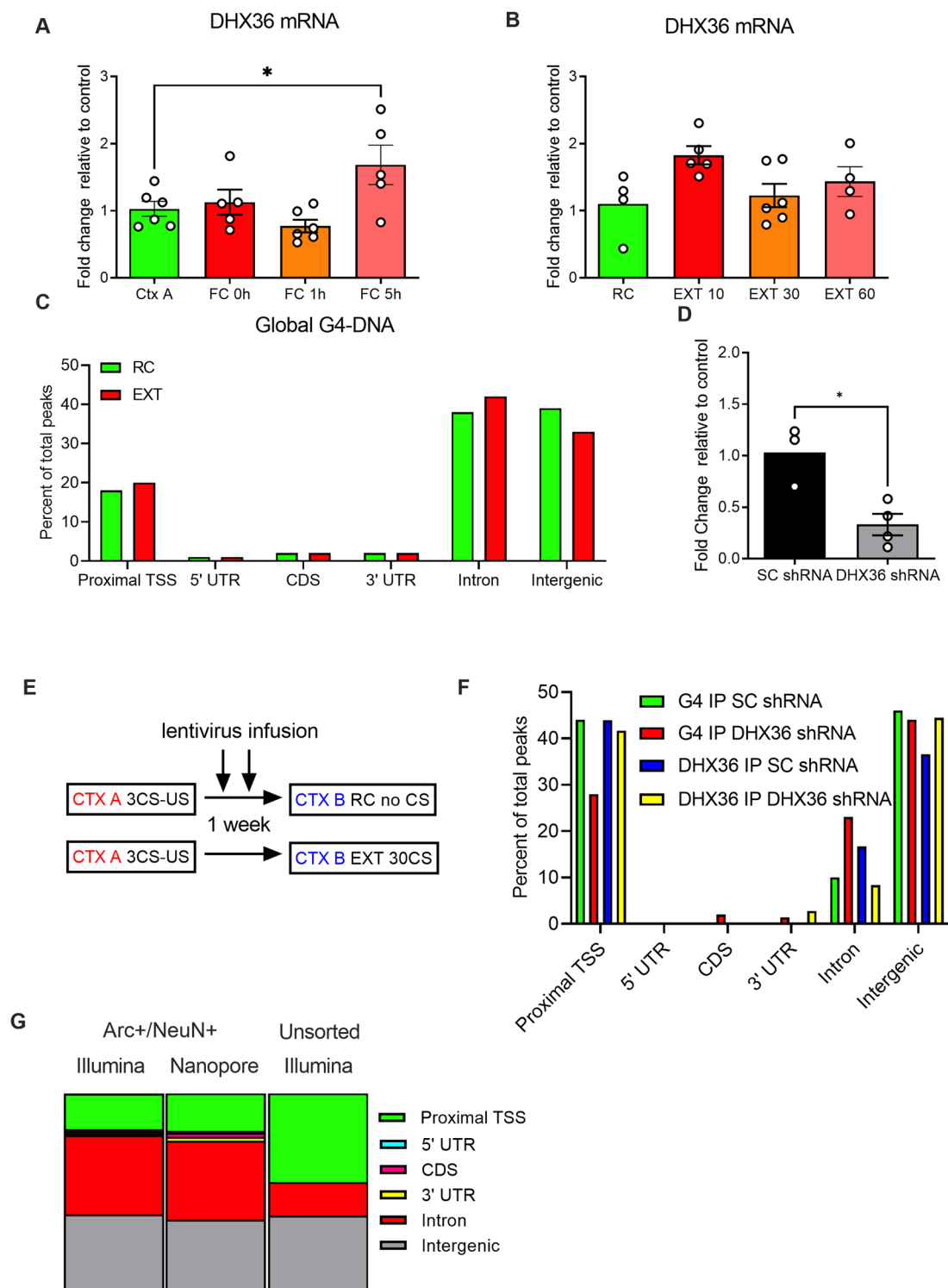


Figure 1. Neuronal genome-wide distribution of G4-DNA and DHX36 is influenced by learning and depends on cell type and activation state. **A**, A total of 48 mice, 6 per group, were either exposed to Context A without conditioning (Ctx A) or FC followed by the mPFC collection performed immediately (FC 0 h), 1 h (FC 1 h), or 5 h posttraining (FC 5 h). There was a significant increase in the expression of the G4-specific helicase DEAH-box helicase 36 (DHX36) in the mPFC at the 5 h time point ($F_{(3,18)} = 4.631$, $*p < 0.05$; Dunnett's post hoc test; Ctx A vs FC 0 h, $p = 0.9601$; Ctx A vs FC 1 h, $p = 0.5920$; Ctx A vs FC 5 h, $*p = 0.0446$). **B**, DHX36 mRNA expression is also transiently induced by fear extinction learning (EXT 10 CS; $F_{(3,15)} = 2.882$, $p = 0.07$; Dunnett's post hoc test; RC vs EXT 10, $*p = 0.0461$). Ctx A, Context A; FC, fear conditioning; EXT, extinction trained; RC, retention control. **C**, Distribution of G4-DNA from RC and EXT mice. 5' untranslated region (5' UTR), proximal TSS (5 kb \pm transcription start site), CDS (coding region), 3' untranslated region (3' UTR). Each bar represents a normalized average (see Extended Data Fig. 1-1 for more details). **D**, Following infusion of a shRNA into the mPFC, a significant decrease in DHX36 mRNA expression was observed ($t_{(5)} = 3.752$, $*p = 0.0133$). **E**, Timeline for training and infusion of lentivirus. **F**, Distribution of G4-DNA and DHX36 in EXT animals treated with SC virus or DHX36 shRNA virus (see Extended Data Fig. 1-1 for more details). **G**, Distribution of G4-DNA in activated and unsorted neurons on the Illumina and Nanopore sequencing platforms (see Extended Data Fig. 1-2 for more details).

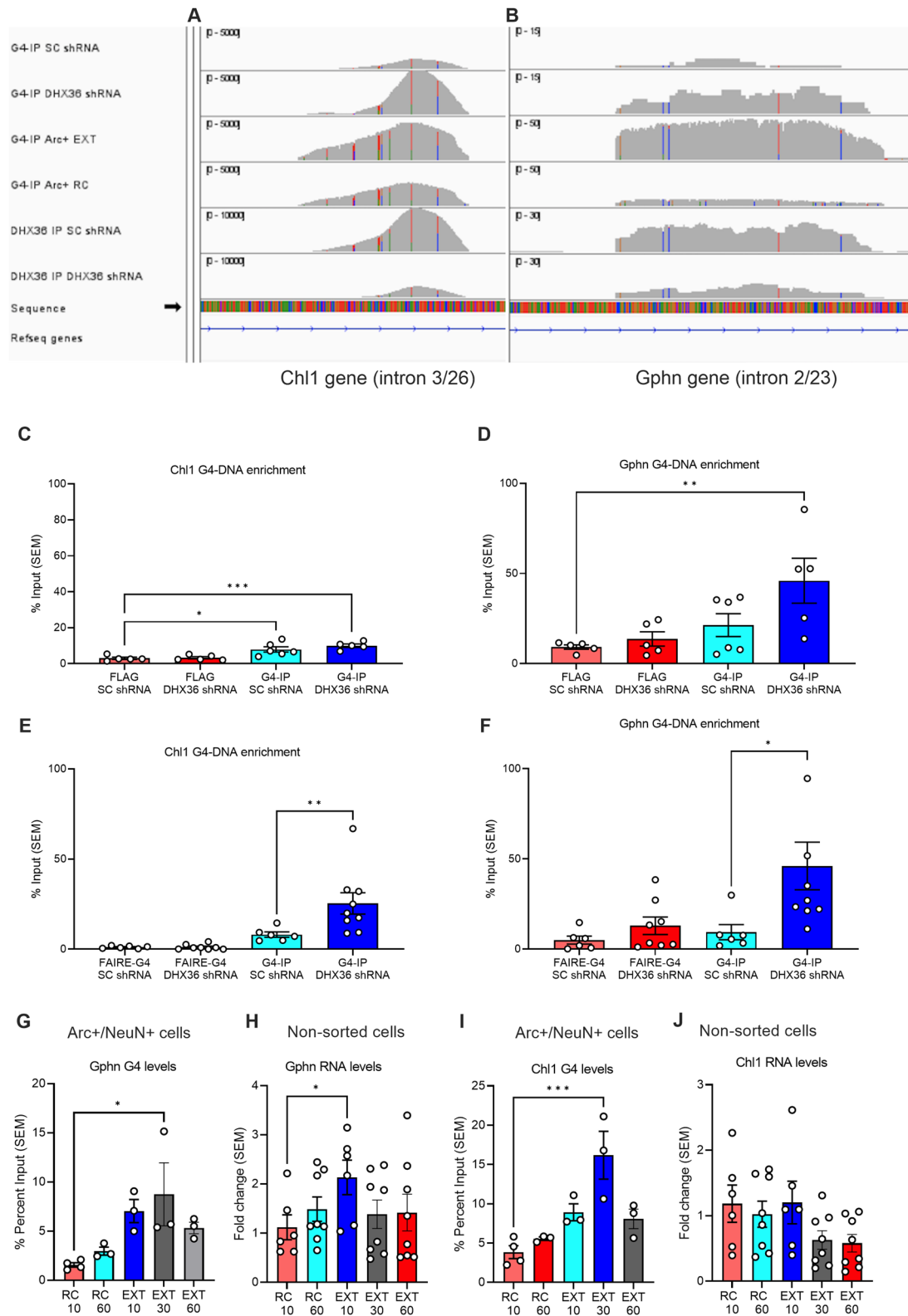


Figure 2. DHX36 regulates the level of G4-DNA at the Gphn and Ch11 locus. Integrated genome browser (IGV) plot of G4-DNA IP with infusions of either DHX36 shRNA or SC shRNA into the mPFC, as well as DHX36 IP for (A) Ch11 loci and (B) Gphn loci. C, Control experiments with FLAG-only controls were performed alongside G4-IP on SC and DHX36 shRNA-treated EXT animals. Analysis at the Ch11 site revealed that there was a significantly higher enrichment in the DHX36-treated G4-IPs but not DHX36-treated FLAG controls ($F_{(3,17)} = 10.68$, $***p < 0.001$; Dunnett's post hoc test; FLAG SC shRNA vs FLAG DHX36 shRNA, $p = 0.9934$; FLAG-G4 SC shRNA vs G4-IP SC shRNA, $**p = 0.093$; FLAG-G4 SC shRNA vs G4-IP DHX36 shRNA, $***p = 0.0007$). Similarly, there was a significant enrichment at the Gphn site only for the G4-IP, not FLAG control ($F_{(3,17)} = 4.900$, $*p < 0.01$; Dunnett's post hoc test; FLAG SC shRNA vs FLAG DHX36 shRNA, $p = 0.9480$; FLAG-G4 SC shRNA vs G4-IP SC shRNA, $p = 0.4913$; FLAG-G4 SC shRNA vs G4-IP DHX36 shRNA, $**p = 0.0072$). SC versus DHX36 shRNA-treated animals that underwent extinction training followed by G4-IP with and without reverse crosslinking were also collected. Without reverse crosslinking, FAIRE allows for the assessment of histone- and protein-free regions. Assessment of the Ch11 gene revealed that much of the G4 peak had protein bound as the signal decreased and was significantly increased following DHX36 shRNA ($F_{(3,25)} = 10.32$, $***p < 0.001$; Dunnett's post hoc test; G4-IP SC shRNA vs FAIRE-G4 SC shRNA, $p = 0.4978$; G4-IP SC shRNA vs FAIRE-G4 DHX36 shRNA, $p = 0.4531$; G4-IP SC shRNA vs G4-IP DHX36 shRNA,

1:20 into 50 mM HEPES, pH 8.8, prewarmed to 45°C. This was injected with a 1 ml syringe and a 25-gauge needle intraperitoneally at least 15 min prior to the onset of behavioral training. At the end of the experiment, the animals were killed, and the brains were then processed as described above, followed by RNA extraction. The RNA was then biotinylated with EZ-Link HPDP-Biotin (Pierce) dissolved in dimethylformamide at a concentration of 1 mg/ml and stored at 4°C. RNA cleanups were performed with TRIzol and Zymo Clean and Concentrator kits as per the manufacturer's recommendations. The RNA was then enriched with streptavidin-linked magnetic Dynabeads C1 (Thermo Fisher Scientific) in the manufacturer's recommended buffers. Elution was performed in binding and wash buffer supplemented with 1% 2-mercaptoethanol, and cleanups were performed again with TRIzol and Zymo columns. To reduce the number of cycles required to amplify the library, and potentially bias the results, we used 16 animals per virus and pooled them into four replicates with 4 animals in each replicate. The RNA was then used with PCR-cDNA sequencing kits (SQK-PCS109) to prepare and sequence the samples. Samples were run on a GridION, with R9.4.1 flow cells. FASTQ files were demultiplexed and trimmed with Guppy (version 4.4.1). Following quality evaluation and additional filtering with Porechop (version 0.2.4), the reads were mapped with Minimap2 (version 2.20) and assembled with StringTie (version 2.1.1). Differential analysis was then performed on transcripts with DESeq2 (version 2.11.40.6).

Native elongation transcript sequencing (NET-seq) and total RNA-seq
The protocol was performed as described by Nojima et al. (2016), with the exception that tissue was first dounced in a glass mortar and pestle. At this point, 10% of the homogenized was taken for total RNA-seq. Thus, RNA was purified from this fraction with TRIzol and Zymo columns according to the manufacturer's protocols. The total RNA was then ribodepleted with the NEBNext rRNA Depletion Kit (NEB) and prepared with the SMARTer Stranded Total RNA-Seq Kit (Takara Bio). The samples were then sequenced on the MiSeq (Illumina), and FASTQ files were obtained for each. These files were evaluated and filtered for quality with FastQC (version 0.73) and Trimmomatic (version 0.38.0), followed by mapping with TopHat (version 2.1.1). Differential analysis was then performed on mapped reads with DESeq2 (version 2.11.40.6).

For the other 90% of the sample, the protocol of Nojima et al. (2016) was followed. This consisted of first fractionating the cell with a nucleus-specific buffer, followed by digestion with MNase, binding with a polymerase II specific antibody (ab817), and enrichment with protein G beads. One alteration to this protocol was to use Nanopore PCR-cDNA sequencing kits (SQK-PCS109) to prepare and sequence the purified RNA samples according to the manufacturer's protocols. Samples were run on a GridION, with R9.4.1 flow cells. FASTQ files were demultiplexed and trimmed with Guppy (version 4.4.1). The reads were then mapped with Minimap2 (version 2.20) and assembled with StringTie (version 2.1.1), and differential analysis was performed with DESeq2 (version 2.11.40.6).

ChIP-seq data analysis

Bioinformatics analysis was performed as previously reported (Marshall et al., 2020). After removing the duplicate reads, low-quality mapping reads and paired-end reads that were not properly aligned, MACS2 (version 2.1.1.20160309) was used to call peaks for each sample using the parameter setting "callpeak -t SAMPLE -c INPUT -f BAMPE-keep-dup = all -g mm -p 0.05 -B". Peak summits identified by MACS2 from all samples were collected to generate a list of potential binding sites. Custom PERL script was then applied to parse the number of fragments (hereafter referred to as counts) that covered the peak

summit in each sample. Each pair of properly paired-end aligned reads covering the peak summit represented one count. The total counts in each sample were normalized before comparison among samples. The potential binding sites were kept if they met all of the following conditions: (1) the sites were not located in the *Mus musculus* (house mouse) genome assembly GRCm38 (mm10) empirical blacklists, and (2) the normalized counts in all three biological replicates in one group were larger than in its input sample, and the normalized counts in at least two replicates were more than twofold larger than in the normalized input count.

Experimental design and statistical analysis

For all animal experiments, we started with a minimum of eight animals per group prior to removal for outliers, surgical complications, or failure to reach behavioral criteria. We also replicated all behavioral experiments twice and pooled animals across these two instances to avoid a single cohort effect potentially driving statistical significance. Due to the fact that the average observed change in fear extinction was 20%, power calculations indicated that a minimum of eight per group was sufficient to determine a statistically significant effect. We have observed effect sizes in the past for genome- and transcriptome-wide changes of 1.2–1.5-fold change or 1–5% of input in approximately 100–200 targets, suggesting that an N of 6 would be sufficiently powered to detect changes. We did not reach this in all cases for the sequencing experiments, and this has been highlighted in the limitations section. For the statistics, one-way and two-way ANOVAs were performed, and when significant a post hoc comparison for all groups to the denoted control group was then performed. For genome-wide and transcriptome-wide experiments following quality control filtering, corrections for pair-wise comparisons were performed. All scripts were run both on a workstation with custom code and Galaxy with the reported version and standard settings so that any pipeline could be replicated by running the pipeline either via Galaxy (<https://usegalaxy.org.au>) or a similar version installed on a workstation.

Results

G4-DNA is regulated by DHX36 during fear and extinction learning

To determine if G4-DNA accumulates in response to fear extinction learning, we fear conditioned 10–16-week-old C57BL/6 mice using a standard tone–shock pairing protocol. We then exposed these mice to either a 10, 30, or 60 CS extinction (EXT) protocol in a novel context or to an equivalent time without re-exposure to the previously CS (RC) and extracted the mPFC after both tasks. An examination of mRNA expression of the G4-DNA helicase DHX36 revealed an increase in DHX36 mRNA 5 h postfear training (Fig. 1A, Extended Data Fig. 1-1) and at 10 CS EXT (Fig. 1B). This suggested an effect of DHX36 on G4-DNA during the late phase of fear consolidation and during extinction learning. G4-DNA sequencing (G4-seq; Hänsel-Hertsch et al., 2018) on DNA derived from mPFC neurons during the early phase of extinction learning (10 CS EXT and RC) revealed that 10 CS EXT training led to a nonsignificant qualitative shift in the percentage of G4-DNA reads 5 kb upstream or downstream of the TSS (proximal TSS) and within introns (Fig. 1C). This was subsequently evaluated quantitatively at the single-gene level.

←

** $p = 0.0098$. **D**, Although the Gphn G4 peak appears to be mainly protein free as there was no decrease in signal in the FAIRE groups, there was also a significant increase in G4 following DHX36 knockdown ($F_{(3,25)} = 1.759$, $p > 0.05$; Dunnett's post hoc test; G4-IP SC shRNA vs FAIRE-G4 SC shRNA, $p = 0.9403$; G4-IP SC shRNA vs FAIRE-G4 DHX36 shRNA, $p = 0.9403$; G4-IP SC shRNA vs G4-IP DHX shRNA, $*p = 0.0234$). **E**, In Arc+/NeuN+ cells extracted from the mPFC after fear and extinction training, there was a significant increase in G4 signal at the Gphn locus during extinction ($F_{(4,11)} = 4.290$, $*p < 0.05$; Dunnett's post hoc test; RC 10 vs EXT 30, $*p = 0.0133$). **F**, There was also a significant increase at this locus for RNA from this Gphn G4 locus in unsorted cells derived from the mPFC following extinction training ($F_{(4,31)} = 1.232$, $*p < 0.05$; Dunnett's post hoc test; RC 10 vs EXT 10, $*p = 0.0437$). **G**, In Arc+/NeuN+ cells extracted from the mPFC after fear and extinction training, there was also a significant increase in G4 signal at the Chl1 locus during extinction ($F_{(4,11)} = 9.907$, $**p < 0.01$; Dunnett's post hoc test; RC 10 vs EXT 30, $***p = 0.0004$). **H**, There was no significant change in RNA expression from the Chl1 G4 locus in unsorted cells derived from the mPFC following extinction training ($F_{(4,31)} = 1.989$, $p = 0.1208$).

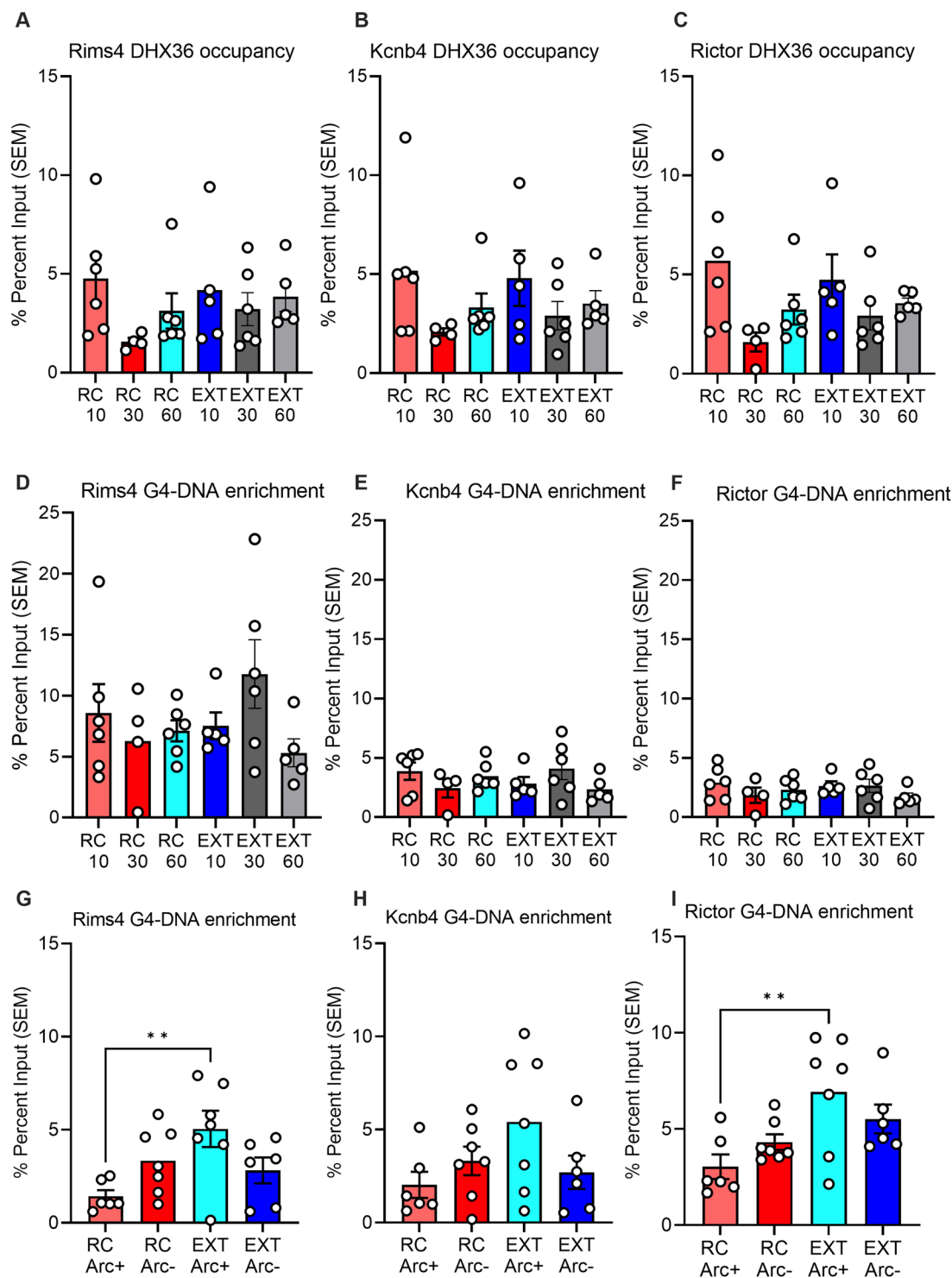


Figure 3. DHX36 and G4-DNA time course for increased G4-DNA targets. DHX36 occupancy in the mPFC following either retention control (RC) or extinction training (EXT) for 10, 30, or 60 conditioned stimuli (10CS, 30CS, 60CS) or equivalent time for RC (RC10, RC30, RC60) with no significant differences observed for (A) Rims4, (B) Kcnb4, and (C) Rictor. There was also no significant change in G4 occupancy following training of the same groups and genes (D) Rims4, (E) Kcnb4, and (F) Rictor. Comparing G4-DNA in activated versus unsorted neurons revealed significant differences between the groups (G). Rims4 (one-way ANOVA $F_{(3,22)} = 4.193$, $**p < 0.01$; Dunnett's post hoc test; RC Arc+ vs EXT Arc-, $**p = 0.0056$). H, Kcnb4 (one-way ANOVA $F_{(3,22)} = 2.118$, $p = 0.1270$). I, Rictor (one-way ANOVA $F_{(3,22)} = 4.421$, $**p < 0.01$; Dunnett's post hoc test; RC Arc+ vs EXT Arc-, $**p = 0.0060$).

To identify G4-DNA regions that were actively regulated during extinction, we designed several shRNA against DHX36. We then used the shRNA which produced the largest significant reduction in DHX36 mRNA for all subsequent experiments (Fig. 1D). Mice were fear conditioned and infused with SC

shRNA or DHX36 shRNA into the ILPFC followed by extinction training (Fig. 1E). We then performed G4-DNA-seq and DHX36 IP-seq (Extended Data Fig. 1-2). The most notable qualitative change in distribution occurred within introns, with DHX36 shRNA increasing the accumulation of G4-DNA and decreasing

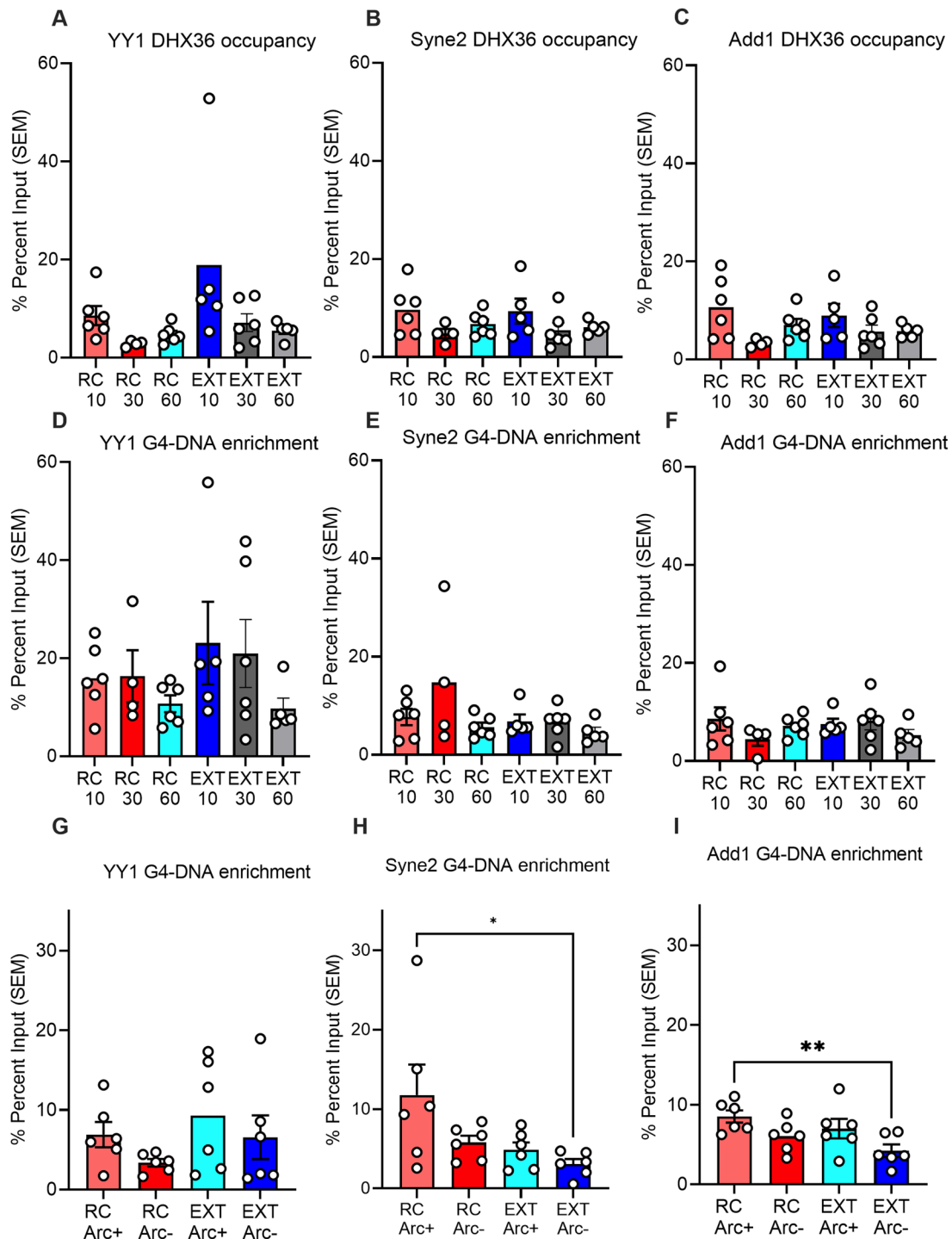


Figure 4. DHX36 and G4-DNA time course for decreased G4-DNA targets. DHX36 occupancy following either retention control (RC) or extinction training (EXT) for 10, 30, or 60 conditioned stimuli (10CS, 30CS, 60CS) or equivalent time for RC (RC10, RC30, RC60) showed a significant increase in (**A**), Yy1 (one-way ANOVA $F_{(5,23)} = 5.254$, $**p < 0.01$; Dunnett's post hoc test; RC10 vs EXT10, $**p = 0.0020$). **B**, Syne2 (one-way ANOVA $F_{(5,23)} = 5.304$, $**p < 0.01$; Dunnett's post hoc test; RC10 vs EXT10, $**p = 0.0018$). **C**, Add1 (one-way ANOVA $F_{(5,23)} = 3.716$, $*p < 0.05$; Dunnett's post hoc test; RC10 vs EXT10, $*p = 0.0190$). There was no significant change in G4 occupancy following training of the same groups and genes (**D**) Yy1, (**E**) Syne2, and (**F**) Add1. However, comparing G4-DNA in activated versus unsorted neurons revealed a significant difference between the groups for (**G**) Yy1 (one-way ANOVA $F_{(3,20)} = 3.382$, $*p < 0.05$; Dunnett's post hoc test; RC Arc+ vs EXT Arc+, $**p = 0.0222$). **H**, Syne2 (one-way ANOVA $F_{(3,20)} = 4.402$, $*p < 0.05$; Dunnett's post hoc test; RC Arc+ vs EXT Arc+, $*p = 0.0227$; RC Arc+ vs EXT Arc-, $**p = 0.0078$). **I**, Add1 (one-way ANOVA $F_{(3,20)} = 5.668$, $**p < 0.01$; Dunnett's post hoc test; RC Arc+ vs EXT Arc+, $*p = 0.0401$; RC Arc+ vs EXT Arc-, $**p = 0.0017$).

DHX36 occupancy within these genomic regions (Fig. 1F). To further identify G4-DNA regulatory sites in neurons, we performed G4-DNA IP, followed by Illumina and Oxford Nanopore sequencing on neurons that had been selectively activated by learning (Extended Data Fig. 1-3). A direct comparison was

made between cells identified as activated neurons based on neuronal nuclei (NeuN) and Arc expression (Arc+/NeuN+ G4-DNA) and unsorted homogenates (with a high proportion of Arc-/NeuN+ neurons). Although the distribution of reads was nearly identical for long-read and short-read sequencing,

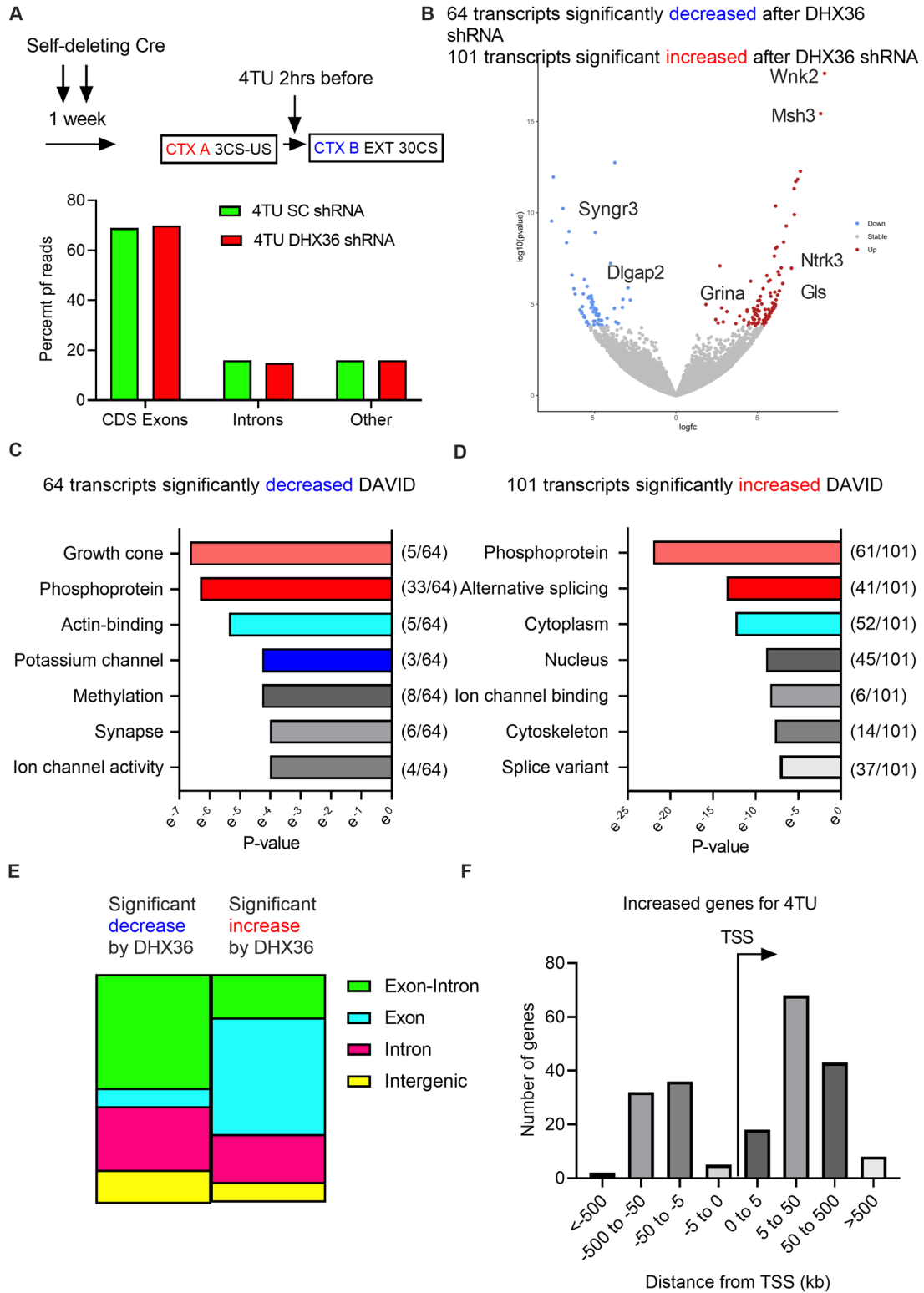


Figure 5. Experience-dependent nascent RNA expression is modulated by G4-DNA. **A**, Timeline of infusions of self-deleting Cre lentivirus, training, and 4TU infusions. Following training, brains from 32 animals were extracted, and RNA was labeled and sequenced, producing a distribution of reads across the transcriptome with the highest amount in the exons. **B**, Volcano plot of 4TU-labeled transcripts that significantly increased or decreased relative to control when DHX36 shRNA was infused (see Extended Data Fig. 5-1 for more details). **C**, Database for Annotation, Visualization and Integrated Discovery (DAVID) plot comparing category to the *p*-value for all of the significantly decreased transcripts (**D**) and all of the significantly increased transcripts. **E**, A visual representation indicating the percentage of 4TU reads from the significantly decreased and increased transcripts which occurred across introns and exons (exon–intron), only over exons (exon), only over introns (intron), or only over intragenic regions (intragenic). **F**, The number of significantly increased 4TU transcripts and their distances in kilobases relative to the closest annotated transcription start site.

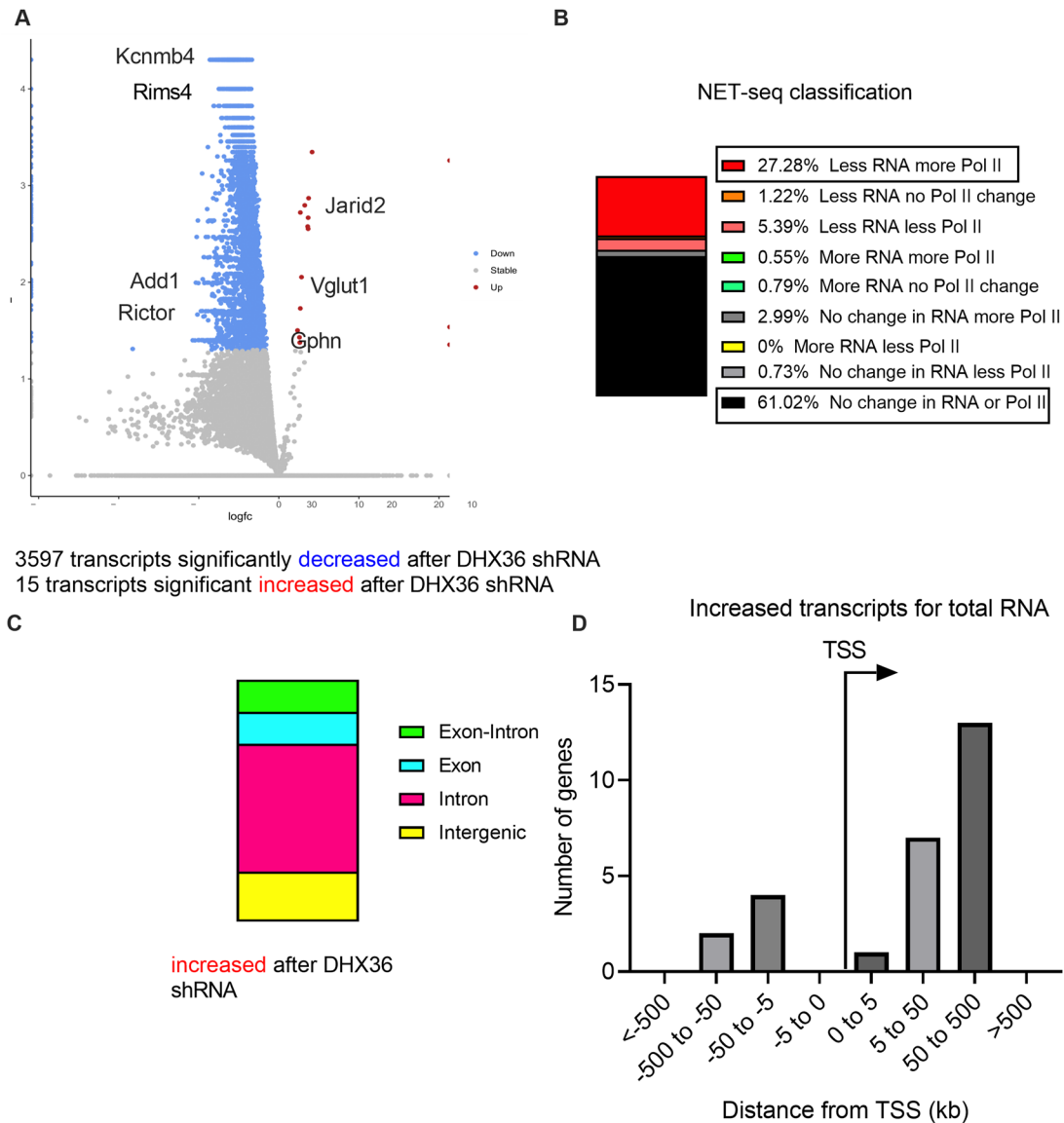


Figure 6. Pol II-associated RNA is influenced by G4-DNA following DHX36 knockdown. **A**, Volcano plot of total RNA expression following infusion of DHX36 shRNA relative to control ($N = 3-4$ per group, which is a pool of 4 animals per biological replicate, a total of 16 animals per virus, 32 total; see Extended Data Fig. 6-1 for more details). **B**, Plot comparing changes in total RNA levels to changes in the amount of Pol II-bound RNA sorted by categories of increasing, decreasing, or no change when comparing control virus to DHX36 shRNA infusion ($N = 3-4$ per group, which is a pool of 4 animals per biological replicate, a total of 16 animals per virus, 32 total; see Extended Data Fig. 6-2 for more details). **C**, A visual representation indicating the percentage of reads from the significantly increased total transcripts (see Extended Data Fig. 6-3 for more details), which occurred across introns and exons (exon-intron), only over exons (exon), only over introns (intron), or only over intragenic regions (intragenic). **D**, The number of significantly increased total transcripts and their distances in kilobases relative to the closest annotated transcription start site.

we observed a nonsignificant qualitatively greater proportion of reads in introns over the proximal TSS in the activated neuron population (Fig. 1G). Together, these data suggest that neuronal activity drives a conformational shift in G4-DNA at the TSS toward the accumulation of G4-DNA within intronic regions.

We next overlapped these data sets in the USC genome browser and the integrated genomics viewer (IGV) to reveal common targets, which had (1) G4-DNA in all three G4-DNA-seq experiments, (2) an increase in G4-DNA when comparing DHX36 shRNA to control, and (3) DHX36 occupancy and a reduction in DHX36 following knockdown. We selected eight targets for validation based on their known association with neuronal plasticity: ying yang 1 (*yy1*), nesprin 2 (*syne2*), adducin 1 (*add1*), regulating synaptic membrane exocytosis 4 (*Rims4*), potassium large conductance calcium-activated channel, subfamily M, β member 4 (*Kcnmb4*), RPTOR independent companion of MTOR, complex

2 (*Rictor*), gephyrin (*Gphn*), and neural cell adhesion molecule L1-like (*Chl1*).

Chl1 and *Gphn* exhibited the most robust G4-DNA signal in introns, with large differences in G4-DNA and DHX36 signal being observed between the two conditions (Fig. 2A,B). To confirm the specificity of these enrichments, we compared G4-DNA signals with and without DHX36 shRNA in FLAG-only controls (FLAG) and those enriched by standard G4-IP. It was found that the G4 signal was significantly higher in DHX36 treated at the *Chl1* and *Gphn* sites (Fig. 2C,D). Additional validation with G4-DNA IP in combination with formaldehyde-assisted isolation of regulatory elements (FAIRE-Seq) revealed an increase in G4-DNA in both genes following the reduction in DHX36 (Fig. 2E,F). These two loci also showed a significant increase in signal in NeuN+/Arc+ cells and a trend in increased RNA expression at these loci in nonsorted cells (Fig. 2G,H). Although G4-DNA and

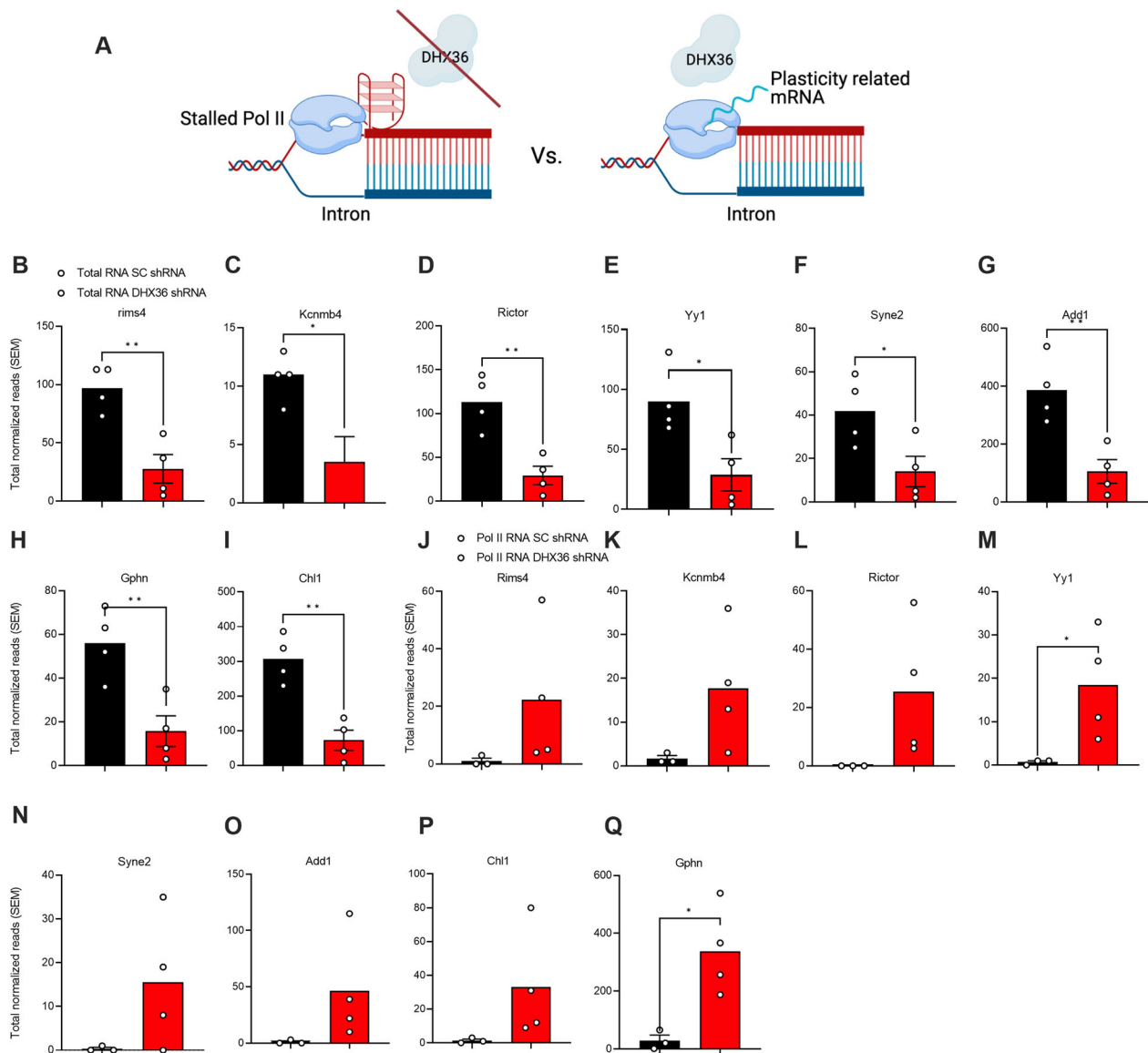


Figure 7. Pol II stalling and RNA expression at selected G4-DNA sites. **A**, Proposed model of G4-DNA and Pol II interaction during transcription associated with memory formation. Comparing total RNA from SC and DHX36 shRNA-treated EXT mice (see Extended Data Fig. 7-1 for more details) showed that there was a significant decrease in **(B)** *Rims4* ($t_{(6)} = 4.416$, $**p < 0.01$), **(C)** *Kcnmb4* ($t_{(6)} = 3.007$, $*p < 0.05$), **(D)** *Rictor* ($t_{(6)} = 4.479$, $**p < 0.01$), **(E)** *Yy1* ($t_{(6)} = 3.135$, $*p < 0.05$), **(F)** *Syne2* ($t_{(6)} = 2.618$, $*p < 0.05$), **(G)** *Add1* ($t_{(6)} = 4.026$, $**p < 0.01$), **(H)** *Chl1* ($t_{(6)} = 5.175$, $**p < 0.01$), and **(I)** *Gphn* ($t_{(6)} = 3.797$, $**p < 0.01$). Pol II-bound RNA increased in **(J)** *Rims4* ($t_{(5)} = 1.448$, $p = 0.1036$), **(K)** *Kcnmb4* ($t_{(5)} = 1.906$, $p = 0.0537$), **(L)** *Rictor* ($t_{(5)} = 1.833$, $p = 0.0631$), **(M)** *Yy1* ($t_{(5)} = 2.451$, $*p < 0.05$), **(N)** *Syne2* ($t_{(5)} = 1.691$, $p = 0.0758$), **(O)** *Add1* ($t_{(5)} = 1.629$, $p = 0.0821$), **(P)** *Chl1* ($t_{(5)} = 1.630$, $p = 0.0820$), and **(Q)** *Gphn* ($t_{(5)} = 3.351$, $*p < 0.05$).

DHX36 binding increased in *Rims4*, *Kcnmb4*, and *Rictor* (Fig. 3A–I) during extinction learning. *Yy1*, *Syne2*, and *Add1* showed the opposite effect, a finding that was most evident in Arc+ activated neurons (Fig. 4A–I). We therefore conclude that G4-DNA is regulated by DHX36 in neurons at genes that are of critical importance for neuronal plasticity and that this occurs in an experience-dependent manner.

DHX36 knockdown transiently increases mRNA expression during extinction learning

It is well established that an increase in G4-DNA, either by stabilizing compounds or by inhibiting G4-DNA helicases such as DHX36, leads to reduced transcription (Kim, 2017). This is thought to occur as a result of G4-DNA impeding the progression of RNA polymerase II (Pol II). In contrast, G4-DNA has also been

shown to enhance transcription when it forms proximal to the TSS, which may occur because of G4-DNA-mediated maintenance of the transcription bubble, which then primes subsequent gene expression (Kim, 2017). To determine which of the two primary models accounts for the G4-DNA-mediated effects on experience-dependent transcriptional activity in neurons, we coinfused a self-deleting Cre recombinase and either SC shRNA or DHX36 shRNA into the ILPFC of mice expressing a Cre-activated UPRT cassette (Kaczmarczyk et al., 2019). To label nascent RNA, 4-TU was infused 2 h prior to exposure to a 30CS EXT protocol, followed by sulfide-mediated click-chemistry enrichment to capture nascent RNAs expressed in response to extinction learning followed by sequencing (Fig. 5A).

A comparison between nascent RNA derived from SC- and DHX36 shRNA-treated mice revealed reduced expression in 64

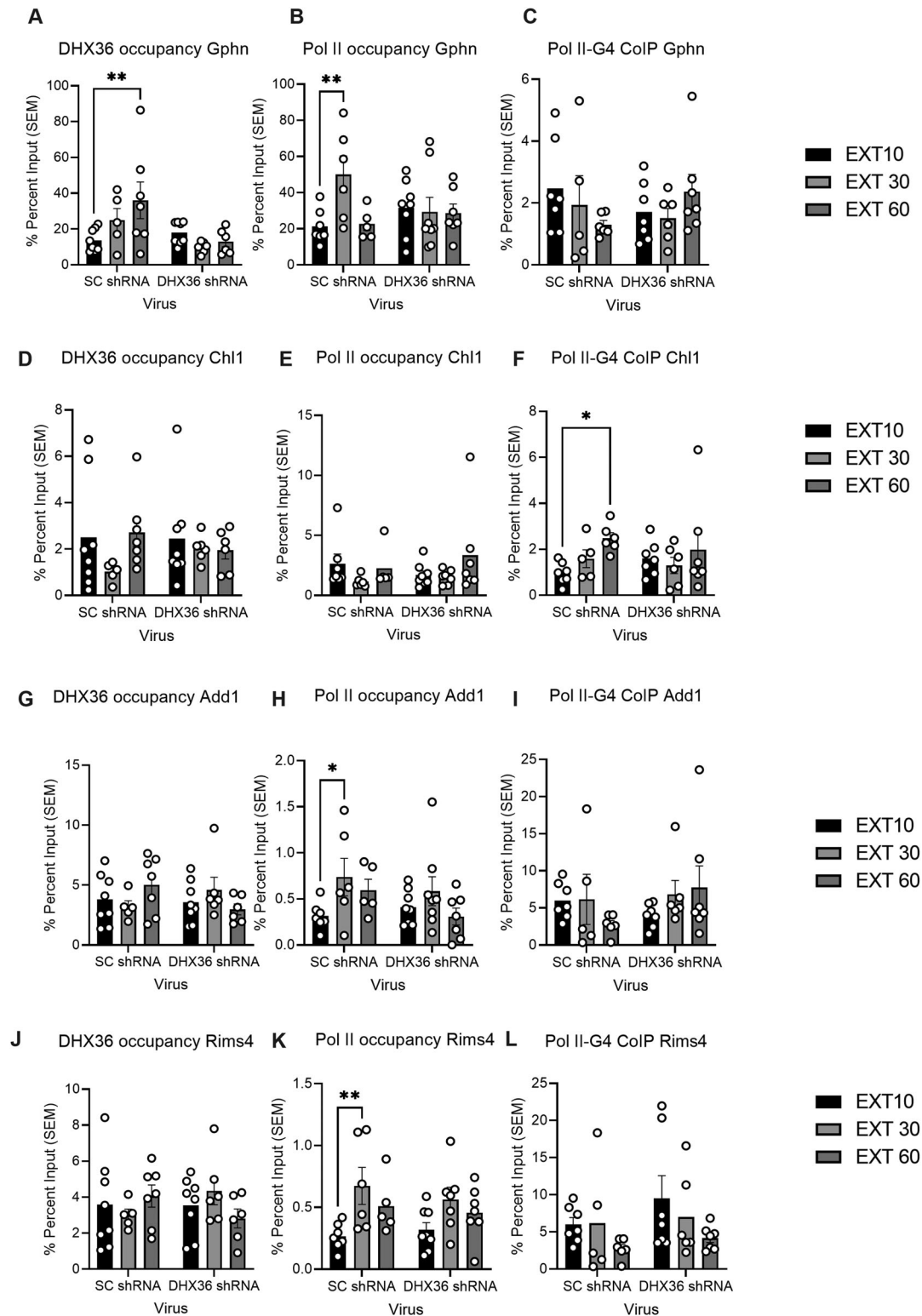


Figure 8. DHX36, Pol II, and G4-Pol II co-occupancy at selected G4-DNA sites. Animals had SC or DHX36 shRNA lentivirus infused into the infralimbic PFC postacquisition as reported in other figures. Their mPFC was then extracted after EXT for 10, 30, or 60 conditioned stimuli (10CS, 30CS, 60CS). From this, it was observed that (**A**) DHX36 occupancy was significantly increased for the SC but not DHX36-treated animals at the Gphn locus ($F_{(2,34)} = 3.983$, $*p < 0.05$; Sidak post hoc test; EXT10 SC vs EXT60 SC, $**p = 0.0057$). (**B**) Pol II occupancy was also significantly increased for the SC but not DHX36-treated animals at the Gphn locus ($F_{(2,34)} = 3.364$, $*p < 0.05$; Sidak post hoc test; EXT10 SC vs EXT30 SC, $**p = 0.0092$). (**C**) There was no significant difference between groups for the CoIP of G4 and Pol II at the Gphn locus. (**D**) For the Chl1 locus, there was no significant change in DHX36 occupancy or (**E**) Pol II occupancy between groups. (**F**) However, there was a significant increase in co-occupancy of G4 and Pol II, only in the SC group ($F_{(2,34)} = 2.838$, $*p < 0.05$; Sidak post hoc test; EXT10 SC vs EXT60 SC, $*p = 0.0363$). For the Add1 locus, there was no significant difference between groups for (**H**) DHX36 occupancy. (**I**) There was a significant increase in Pol II occupancy only for the SC group though ($F_{(2,34)} = 2.838$, $*p < 0.05$; Sidak post hoc test; EXT10 SC vs EXT30 SC, $*p = 0.0468$). (**J**) There were no significant changes in the co-occupancy of G4 and Pol II. (**K**) For the Rim4 locus, there was no significant change in DHX36 occupancy. (**L**) However, there was a significant increase in Pol II occupancy, only in the SC group ($F_{(2,34)} = 2.838$, $*p < 0.05$; Sidak post hoc test; EXT10 SC vs EXT30 SC, $**p = 0.0068$).

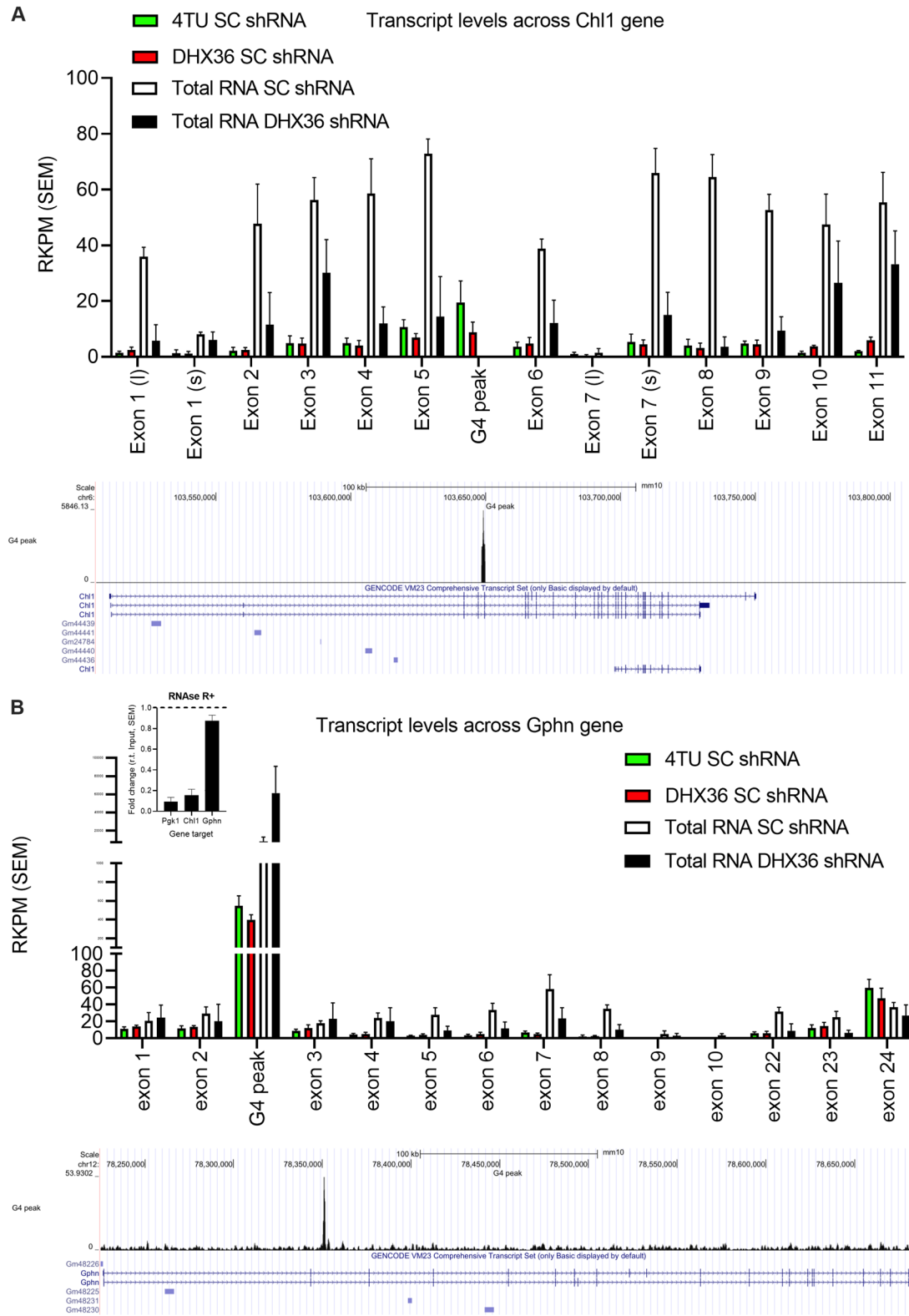


Figure 9. Chl1 and Gphn total and nascent RNA overlap with G4-DNA sites. Integrated genome browser (IGV) showing the reads per kilobase million (RPKM) derived from total RNA sequencing (total RNA) and 4TU metabolic labeling sequencing of mice treated with either SC or DHX36 shRNA. Data are across each exon of the gene relative to the G4 peak for (A) Chl1 and (B) Gphn. In addition to this change in nascent versus total RNA, we also observed that the Gphn locus alone was resistant to RNase R.

genes following DHX36 knockdown, whereas 101 transcripts were found to increase (Fig. 5B and Extended Data Fig. 5-1). Gene ontology analysis revealed that transcripts related to neuronal processes such as ion channels and actin binding were

reduced (Fig. 5C). In contrast, increased expression was found in genes associated with alternative splicing as well as genes that are known to regulate ion channel binding (Fig. 5D). Further, decreased RNA expression mostly occurred across

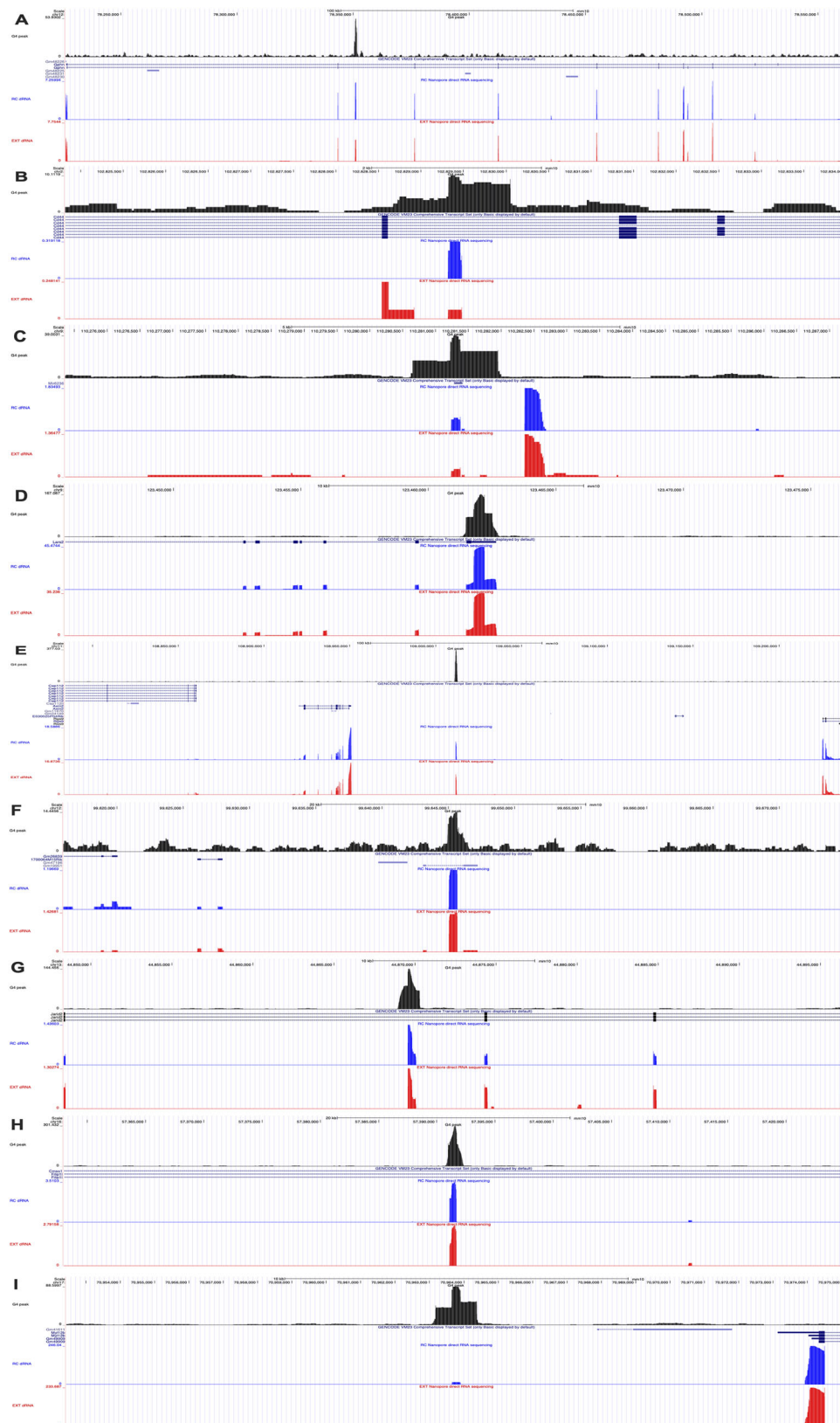


Figure 10. Examples of sites of G4-DNA and significant changes in RNA across the transcriptome. Integrated genome browser (IGV) traces of the G4-DNA peak, as well as RNA expression across a variety of genomic loci including (A) Gphn, (B) Cd44, (C) Mir6236, (D) Lars2, (E) Intragenic site 1, (F) Gm19951, (G) Jarid2, (H) Cms1, and (I) Intragenic site 2.

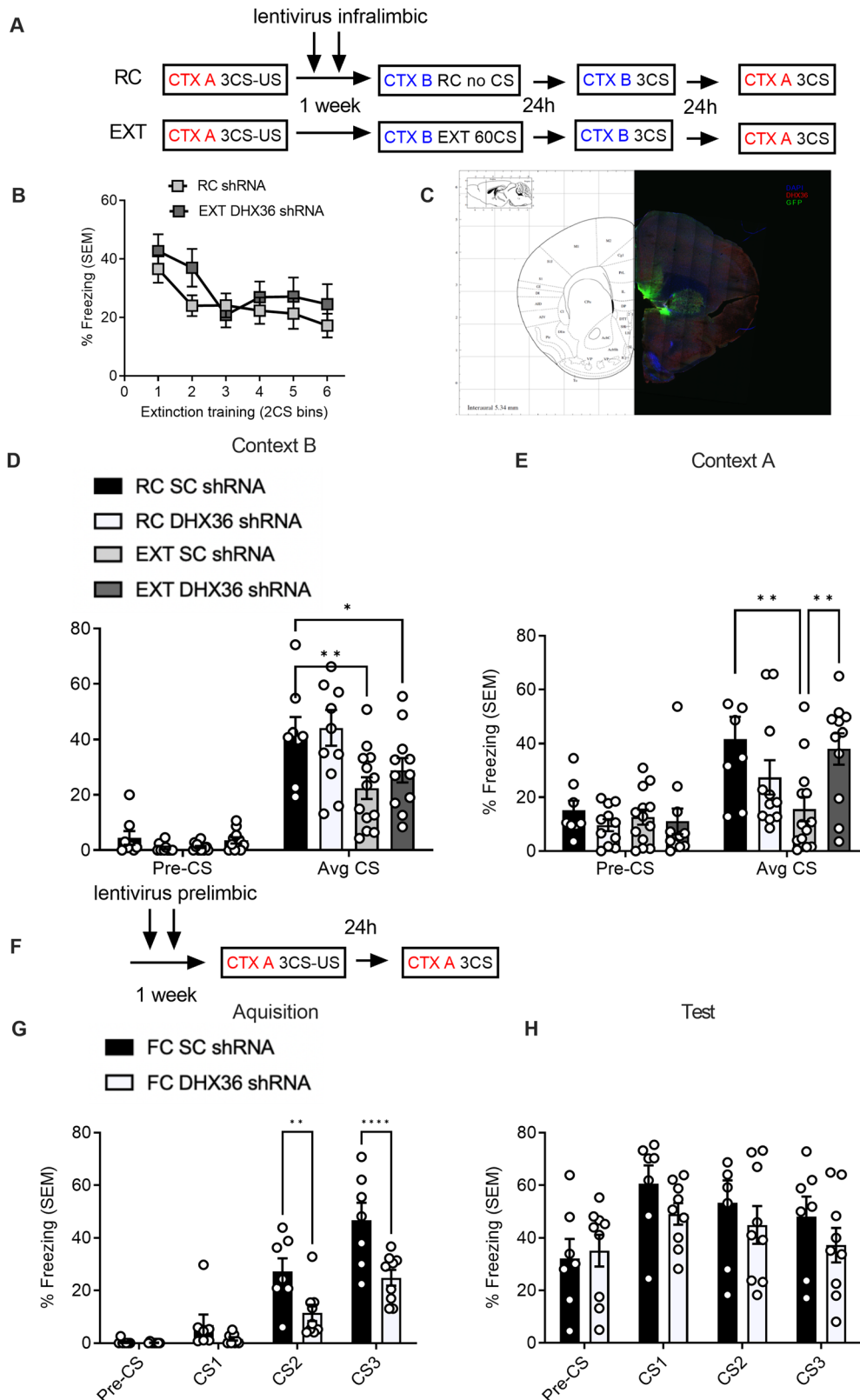


Figure 11. G4-DNA is required for both fear extinction and fear acquisition. **A**, Timeline of training and **(B)** within-session extinction training. There was no significant difference between groups. **C**, Visual representation of infusion of virus into infralimbic PFC with some viral spread outside of target zone. **D**, These infusions did not lead to a significant impairment in memory for fear extinction following a 60 CS training protocol in Context B as both groups showed a significant reduction in comparison with RC SC ($n = 8$ /group, one-way ANOVA $F_{(3,39)} = 4.466$, $*p < 0.01$, Sidak post hoc test; RC scrambled shRNA vs EXT scrambled shRNA, $**p = 0.0034$; Holm–Sidak; RC SC shRNA vs EXT DHX36 shRNA, $**p = 0.0034$; EXT, extinction trained; RC, retention control; Avg CS, average of 3 CS exposures). **E**, DHX36 shRNA did lead to a significant impairment in expression of extinction memory in Context A following a 60 CS training protocol in Context B ($n = 8$ /group, two-way ANOVA $F_{(3,39)} = 5.0390$, $*p < 0.05$, Sidak post hoc test; RC scrambled shRNA vs EXT scrambled shRNA, $**p = 0.01$; EXT scrambled shRNA vs EXT DHX36 shRNA, $*p = 0.0492$). **F**, Timeline of training and infusion **(G)** of DHX36 shRNA into the prelimbic PFC. This led to a significant impairment in acquisition ($n = 8$ /group, two-way ANOVA, $F_{(3,56)} = 4.335$, $p < 0.0001$, Sidak post hoc test; FC Scrambled vs FC DHX36, CS2, $**p = 0.0056$; CS3, $****p < 0.0001$). **H**, However, there was no significant difference between the two groups at the test in Context A.

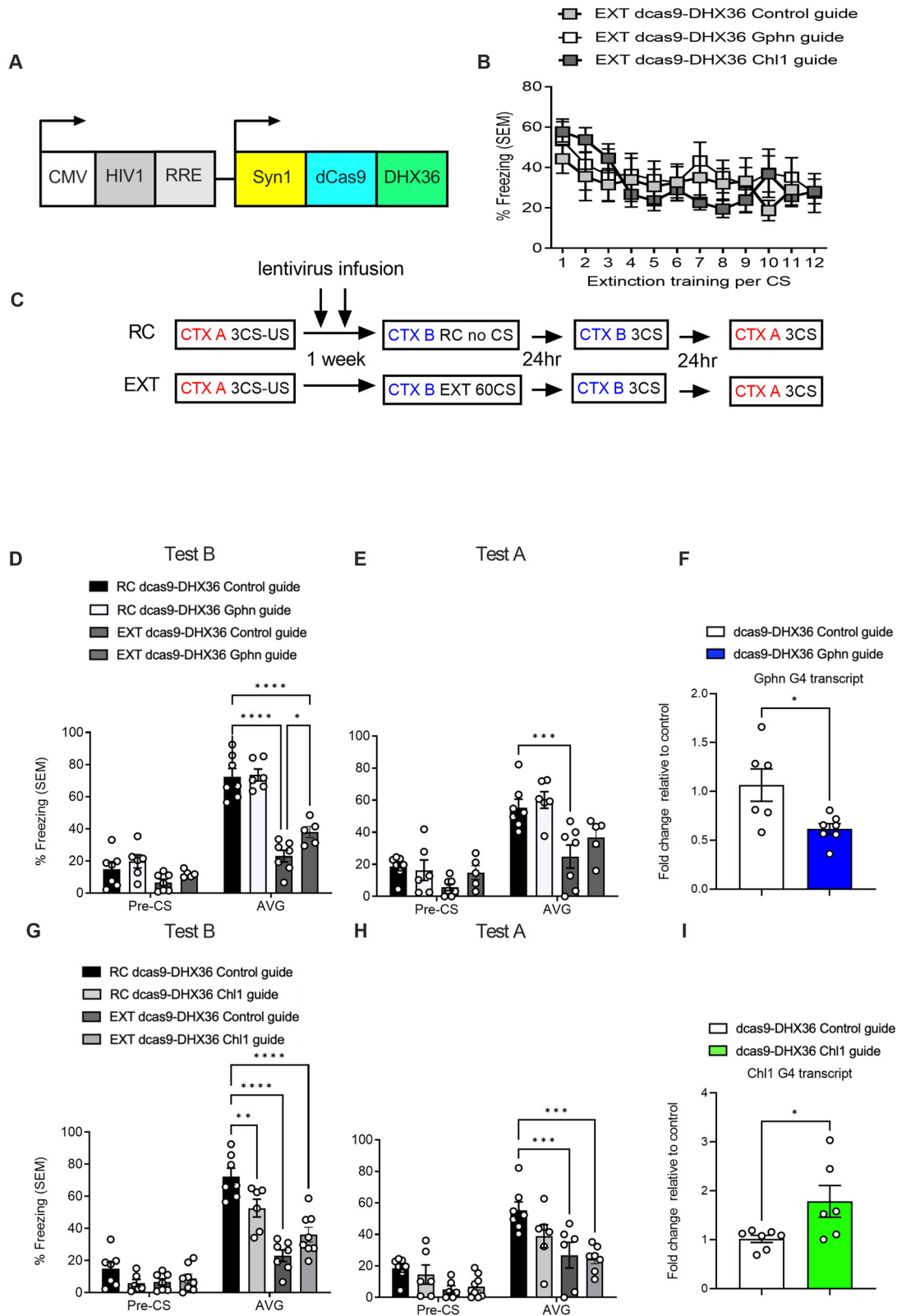


Figure 12. Targeted resolution of G4-DNA at the Ch1 and Gphn locus impairs memory. **A**, Design of the lentiviral construct CRISPR-dCas9-DHX36. **B**, Infusions of the constructs had no significant effect on within-session extinction learning. **C**, Timeline of training and lentivirus infusion into the ILPFC of a CRISPR-dCAS9-DHX36. This construct was directed to either a control or Gphn locus. **D**, It led to a significant impairment in memory for fear extinction following a 60 CS training protocol in Context B as there was a significant difference between the two EXT groups ($n = 6-8/\text{group}$, two-way ANOVA, $F_{(3,21)} = 26.19$, $p < 0.0001$, Tukey's post hoc test; RC dCas9-DHX36 control guide vs EXT dCas9-DHX36 control guide, $***p < 0.0001$; RC dCas9-DHX36 control guide vs EXT dCas9-DHX36 Gphn guide, $***p < 0.0001$; EXT dCas9-DHX36 control guide vs EXT dCas9-DHX36 Gphn guide, $*p = 0.0453$). **E**, Furthermore, in Context A, only the control EXT group showed significant reduction ($n = 6-8/\text{group}$, two-way ANOVA, $F_{(3,21)} = 7.225$, $p = 0.0016$, Tukey's post hoc test; RC dCas9-DHX36 control guide vs EXT dCas9-DHX36 control guide, $***p = 0.0003$). **F**, CRISPR-dCAS9-DHX36 directed to the Gphn locus led to a significant decrease in mRNA expression ($n = 7/\text{group}$, t test $t_{(11)} = 2.76$, $*p < 0.05$). **G**, Lentivirus infusion

larger sections of the gene as indicated by a higher percent of significant reads in exon–intron spanning regions, whereas the increase in nascent RNA expression was detected primarily over exons (Fig. 5E). To determine whether the effect on transcription was the result of G4-DNA stabilization of the transcription bubble around the TSS, we analyzed the overlap between the regions of increased transcription, G4-DNA sites, and TSS (identified by altTSS), revealing a bias toward increases upstream rather than downstream of the TSS (Fig. 5F). These data suggest that, in the context of fear extinction learning, the accumulation of G4-DNA is associated with both reduced and increased nascent RNA expression and that this occurs along a very short-term temporal scale.

G4-DNA promotes polymerase II stalling within learning-related genes

Because nascent RNA-seq using metabolic labeling with 4-TU is more likely to detect regulatory mechanisms associated with enhanced transcription by sampling nascent RNA expression in a narrow temporal window, we next wanted to assess potential polymerase stalling related to G4-DNA transcriptional regulation. A separate cohort of animals was infused with SC and DHX36 shRNA followed by a 30CS EXT protocol. The mPFC was extracted posttraining and subjected to both total RNA-seq and NET-seq, which enabled the quantification of Pol II–associated RNA and a comparison between total RNA and the binding of transcripts to Pol II in the same animal (Nojima et al., 2016). Overall, we observed a significant reduction in transcripts following DHX36 shRNA treatment when sampling total RNA (Fig. 6A and Extended Data Fig. 6-1). Although most transcripts exhibited no change in RNA levels or Pol II occupancy (Fig. 6B), 27% of genes exhibited a decrease in RNA expression (in the total RNA fraction) with a concomitant increase in Pol II binding (in the Pol II fraction, Extended Data Fig. 6-2). Further, in comparison with nascent RNA-seq, the few transcripts that increased following DHX36 shRNA treatment were more likely to be introns (Fig. 6C). However, there was a bias for the increase to occur upstream of the TSS, again supporting the interpretation that increased RNA expression may be governed by G4-DNA maintenance of the transcription bubble (Fig. 6D; Extended Data Fig. 6-3). Overall, these results indicate that stable G4-DNA sites primarily act as gene silencers in neurons. It also suggested that Pol II stalling had occurred in genes where G4-DNA accumulated but was not removed (Fig. 7A). In fact, we observed a significant decrease in total RNA and a significant increase in the fraction of RNA associated with Pol II within all eight of the validated G4-DNA targets (Fig. 7B–Q and Extended Data Fig. 7-1).

We then performed Pol II ChIP-qPCR, as well as Pol II-G4 CoIP-qPCR, on four of the targets that were significantly enriched for G4. Gphn, Add1, and Rims4 all showed significant changes in Pol II occupancy that were dependent on DHX36 shRNA, despite only Gphn showing a significant change in DHX36 occupancy at the level of DNA (Fig. 8A–L). These data suggest that, in conjunction with the known role of

DHX36 in targeting both RNA and DNA, DHX36 knockdown may influence other processes beyond DHX36 occupancy at G4-DNA sites. However, there was a significant change in Pol II-G4 occupancy at Chl1 and a trend for DHX36 alteration and Pol II at the level of single IP (Fig. 8A–L), suggesting that G4-DNA is driving a Pol II change at this and other targets but that this may be masked by the nonspecificity of the manipulation and lack of cell type specificity during the IP. This is why for subsequent experiments investigating Chl1 and Gphn manipulation, we built a neuron- and locus-specific, DHX36-dCas9 construct.

Novel targets for G4-DNA-mediated transcriptional regulation

Our transcriptome-wide data provided support for both models of transcriptional regulation by G4-DNA. To further explore the role of G4-DNA in experience-dependent gene regulation, we next used a gene-specific analysis of changes in RNA expression. A manual reanalysis of every significantly altered gene in the transcriptome-wide data, by examining each gene coordinate into the USC genome browser and overlapping it with the G4-DNA peak data, as well as our own and previously published data sets, revealed many other examples (Fig. 9A,B). The RNA products overlapping with G4-DNA did not appear to share a common subtype, as some occurred over annotated and putative long noncoding RNAs, as well as microRNAs, whereas the Gphn locus appeared to encode a circular RNA as evidenced by its resistance to RNase R treatment (Fig. 9B). Together, these findings suggest that although increased RNA expression can be explained by G4-DNA being maintained proximal to the TSS, and decreased RNA expression is associated with Pol II stalling, both short- and long-term changes in G4-DNA are also associated with a novel subclass of noncoding RNAs, the functional relevance of which remains to be investigated (Fig. 10A–I).

DHX36 is required for the consolidation of fear extinction memory

Having established that G4-DNA has a significant impact on transcription we next sought to investigate its effect on learning and memory, in vivo. Specifically, to determine if G4-DNA regulates memory stability, we infused DHX36 shRNA into the ILPFC of mice immediately after fear training, followed by fear extinction training a week later and two tests in both the original context (A) and extinction context (B; Fig. 11A). DHX36 shRNA had no effect on within-session extinction learning (Fig. 11B) when expressed in the infralimbic PFC after FC (Fig. 11A,C); however, extinction memory was impaired in both contexts (Fig. 11D,E). A separate cohort of animals was infused with SC and DHX36 shRNA into the prelimbic region of the mPFC (Fig. 11F), which is known to regulate the acquisition and consolidation of fear memory. Curiously, DHX36 shRNA led to a significant impairment in the acquisition of cued fear (Fig. 11G) but had no significant effect on expression at the test (Fig. 11H).

←

into the infralimbic PFC of a CRISPR-dCas9-DHX36 construct directed to either a control or Chl1 locus led to a significant reduction in the expression of the original fear memory in Context B with no impairment of extinction ($n = 6$ –8/group, two-way ANOVA, $F_{(3,24)} = 15.67$, $p < 0.0001$, Tukey's post hoc test; RC dCas9-DHX36 control guide vs EXT dCas9-DHX36 control guide, $***p < 0.0001$; RC dCas9-DHX36 control guide vs EXT dCas9-DHX36 Chl1 guide, $***p < 0.0001$; RC dCas9-DHX36 control guide vs RC dCas9-DHX36 Gphn guide, $**p = 0.0071$). **H**, In Context A, there was no significant impairment of expression of original fear or the extinction memory by Chl1-DHX36-dCas9 ($n = 6$ –8/group, two-way ANOVA, $F_{(3,24)} = 7.26$, $p < 0.0001$, Tukey's post hoc test; RC dCas9-DHX36 control guide vs EXT dCas9-DHX36 control guide, $***p = 0.0008$; RC dCas9-DHX36 control guide vs EXT dCas9-DHX36 Chl1 guide, $***p = 0.0001$). **I**, CRISPR-dCas9-DHX36 directed to the Chl1 locus led to a significant increase in mRNA expression ($n = 6$ /group, t test $t_{(11)} = 2.48$, $*p < 0.05$).

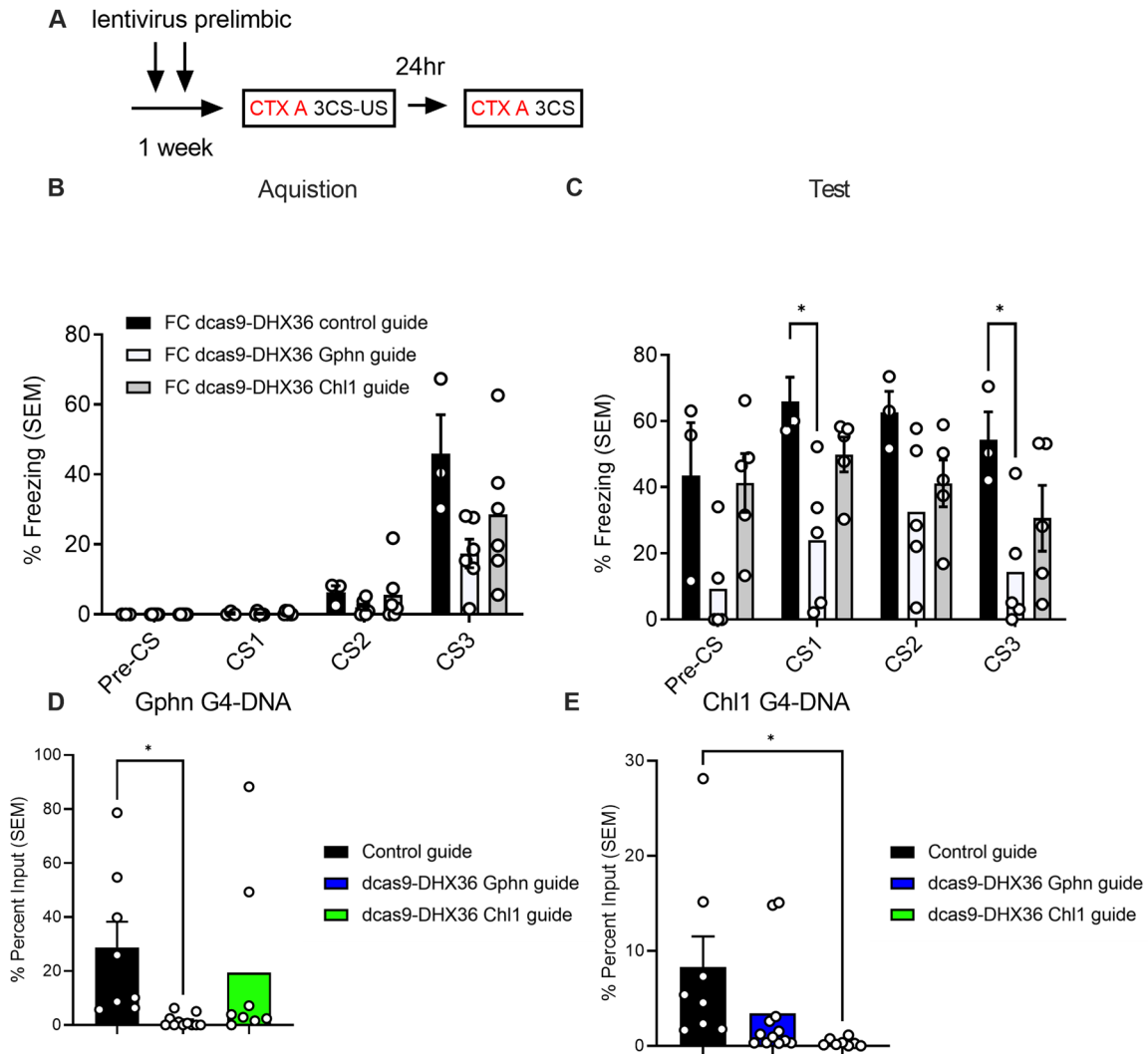


Figure 13. Targeted resolution of G4-DNA by DHX36-dCas9 in the prelimbic cortex impairs fear memory. **A**, Pictorial of timeline for behavioral training and lentivirus infusion into the prelimbic region of the prefrontal cortex. **B**, After infusion of dCas9-DHX36 lentivirus into the prelimbic PFC, there was no significant impairment in acquisition for the Gphn or Chl1 guide. **C**, However, there was a significant impairment in recall for the Gphn guide in Context A ($F_{(2,11)} = 17.31$, $**p < 0.01$; Dunnett's post hoc test; CS1 control guide vs Gphn guide, $*p = 0.0209$; CS3 control guide vs Gphn guide, $*p = 0.0298$; CS3 control guide vs Gphn guide, $***p = 0.0002$). **D**, In addition, following infusion of dCas9-DHX36 with either control guides, Gphn guides, or Chl1 guides, there was a significant reduction in G4-DNA at the Gphn locus following Gphn guide infusion ($F_{(2,24)} = 3.574$, $*p < 0.05$; Dunnett's post hoc test; control guide vs Gphn guide, $*p = 0.0322$). **E**, There was also a significant reduction in G4-DNA at the Chl1 locus with the Chl1 guides ($F_{(2,24)} = 3.375$, $*p < 0.05$; Dunnett's post hoc test; control guide vs Chl1 guide, $*p = 0.0322$).

Together these data suggest that preventing the removal of G4-DNA impairs memory processes.

Targeted reduction in G4-DNA regulates fear memory, depending on the gene target

One limitation of manipulating DHX36 is that it targets G4-RNA as well as G4-DNA. To overcome this issue and more directly define a role for DHX36 in the regulation of G4-DNA in neurons, we designed a synapsin 1-driven dCas9-DHX36 construct (Fig. 12A), which can be directed to specific genomic loci to drive the resolution of G4-DNA and expressed these constructs with lentivirus after FC selectively in neurons. We selected Gphn and Chl1 based on their known roles in plasticity and memory and our observation of a learning-induced role for G4-DNA-mediated effects on gene expression at these loci. We found no effect of dCas9-DHX36 at the Gphn locus on within-session extinction (Fig. 12B); however, following our standard infusion timeline

(Fig. 12C), we found that extinction memory was significantly impaired (Fig. 12D,E), and it led to a significant reduction in Gphn RNA at this locus (Fig. 12F). In contrast, although there was no effect on within-session extinction when Chl1 was targeted by dCas9-DHX36, a significant reduction in fear expression in the Chl1-RC group was found (Fig. 12G,H), and a significant increase in transcription at this G4-DNA site was observed (Fig. 12I). We then performed a second experiment where dCas9-DHX36 was infused prior to fear learning. Although targeting DHX36 to the Chl1 locus led to a modest effect on fear during acquisition and retrieval, the same manipulation at the Gphn locus produced significant impairment for the expression of cued fear (Fig. 13A–C). These constructs also showed a significant reduction of G4-DNA signal at their respective target sites (Fig. 13D,E). Together, these data confirm that G4-DNA serves to regulate learning-induced gene expression in a state-dependent and gene-specific manner, which can have opposing effects depending on the phase of memory formation.

Discussion

The accumulation of G4-DNA has classically been associated with telomere maintenance (Henderson et al., 1987) and, more recently, with class-switch recombination in immune cells (Qiao et al., 2017). Although it has been previously observed in neurons, it was thought to reflect genome instability and DNA damage (Clark et al., 2012) and autophagy (Lejault et al., 2020; Moruno-Manchon et al., 2020). Here, we have found that G4-DNA is regulated by DHX36 in genes with known roles in neuronal plasticity, with the most pronounced effects occurring in introns. Thus, although persistent G4-DNA may produce damage and impaired transcription in some cell types, it is also involved in neural plasticity and appears to be temporally regulated by DHX36, implying a role for G4-DNA-specific binding proteins and helicases in neurons (Kang and Henderson, 2002; Zhang et al., 2021). In this respect, DHX36 regulates G4-DNA primarily in the TSS and introns in neurons, whereas in immune cells, BMI1 promotes the accumulation of G4-DNA and subsequent regulation of L1-containing transcripts, suggesting that different G4-DNA-related binding proteins may regulate different subregions of the genome (Hanna et al., 2021).

G4-DNA has been linked to decreased RNA expression by disrupting Pol II readthrough (Robinson et al., 2021). We also observed robust decreases in total RNA, which were accompanied by the accumulation of Pol II following an increase in G4-DNA by DHX36 knockdown. This provides further support for the effect of Pol II RNA stalling on RNA expression and extends this to include neurons involved in fear and extinction learning. We also found that G4-DNA promotes the expression of specific transcripts both downstream of G4-DNA and directly at this site. These observations, in combination with the changes in G4-DNA induced by DHX36 at different time points for different genes, imply an activity-regulated switch such that G4-DNA, if stabilized, can inhibit transcription on a long-term timescale, followed by rapid initiation of transcription following targeted release of G4-DNA. This is supported by our data on the *Gphn* gene locus whereby extended G4-DNA following DHX36 knockdown resulted in a global reduction of *Gphn*, that is, robust neuronal activity increased G4-DNA and reduced RNA expression with subsequent behavioral training or weak depolarization, leading to G4-DNA release and the triggering of transcription. These data further highlight the need to better understand the mechanisms underlying G4-DNA formation, stability, and resolution across a variety of cell types and activity states.

It is evident that G4-DNA regulation is required for memory processes. Although we observed no effect on fear extinction learning when G4-DNA was increased in the ILPFC, the consolidation of fear extinction memory was impaired. One caveat is that the manipulation of DHX36 can also influence G4-RNA. Therefore, using the dCas9 system, we manipulated G4-DNA at the *Gphn* and *Chl1* loci, respectively, finding that both led to significant changes in RNA expression associated with the G4-DNA and influenced learning and memory. Target resolution of G4-DNA at the *Chl1* locus led to impaired fear memory, whereas the same manipulation at the *Gphn* locus impaired fear extinction memory. Subsequent manipulations prior to the acquisition of fear further confirmed that a DHX36-mediated reduction in G4-DNA at the *Gphn* locus directly affects fear acquisition. These findings suggest a switch-like influence of G4-DNA on transcription as either chronically stabilizing G4-DNA by reducing DHX36 or constitutively reducing G4-DNA by driving DHX36

to specific sites along the genome, leading to overall impairments in memory.

In summary, we have discovered that G4-DNA is directly involved in modulating fear-related memory and that the global model for the regulation of transcription by G4-DNA is dependent on both the cell type and its activation state. Historically, the accumulation of G4-DNA in neurons has been thought to reflect DNA damage and impaired transcriptional activity; however, when G4-DNA is temporally restricted by DHX36, it clearly plays a permissive role in experience-dependent neuronal plasticity. G4-DNA is therefore a critical molecular switch underlying the regulation of neuronal transcription and the consolidation of memory.

Limitations

Due to the use of the commercially available G4-DNA antibody first developed by the Balasubramanian laboratory, instead of the more recently developed G4-DNA cut and run, or Chem-map protocols, our data may have a higher rate of false negatives and positives than more recent data sets on G4-DNA. The absence or presence of targets within other neuronal subtypes or brain regions should be evaluated further before acceptance of the generality of these findings in neurons. Furthermore, due to the fact that neuron and non-neurons, as well as activated versus nonactivated cells were not directly compared genome-wide, conclusions about G4 localization (i.e., intron, exon, TSS) changes due to cell type or state will require further investigation. In addition, although the gene-specific targeting of the DHX36-dCas9 construct was neuron specific, some observations contained in this paper may not be limited to neurons as the DHX36 shRNA we used was not neuron specific. A control construct with a point mutation in the helicase domain is also being developed for future experiments to enhance specificity. Further, due to input limitations, apart from the G4-DNA NeuN+/Arc+ FACS sorting experiment and subsequent qPCR validation, sequencing was performed on unsorted tissue from the mPFC, which may obscure interpretation.

Data Availability

All data are available in the main text, the extended data, or by reasonable request.

References

- Alberini CM (2009) Transcription factors in long-term memory and synaptic plasticity. *Physiol Rev* 89:121–145.
- Bredy TW, Wu H, Crego C, Zellhoefer J, Sun YE, Barad M (2007) Histone modifications around individual BDNF gene promoters in prefrontal cortex are associated with extinction of conditioned fear. *Learn Mem* 14:268–276.
- Bruel-Jungerman E, Rampon C, Laroche S (2007) Adult hippocampal neurogenesis, synaptic plasticity and memory: facts and hypotheses. *Rev Neurosci* 18:93–114.
- Campbell RR, Wood MA (2019) How the epigenome integrates information and reshapes the synapse. *Nat Rev Neurosci* 20:133–147.
- Chen MC, Tippiana R, Demeshkina NA, Murat P, Balasubramanian S, Myong S, Ferré-D'amaré AR (2018) Structural basis of G-quadruplex unfolding by the DEAH/RHA helicase DHX36. *Nature* 558:465–469.
- Clark DW, Phang T, Edwards MG, Geraci MW, Gillespie MN (2012) Promoter G-quadruplex sequences are targets for base oxidation and strand cleavage during hypoxia-induced transcription. *Free Radic Biol Med* 53:51–59.
- Gräff J, et al. (2014) Epigenetic priming of memory updating during reconsolidation to attenuate remote fear memories. *Cell* 156:261–276.
- Hanna R, Flamier A, Barabino A, Bernier G (2021) G-quadruplexes originating from evolutionary conserved L1 elements interfere with neuronal gene expression in Alzheimer's disease. *Nat Commun* 12:1828.

- Hänsel-Hertsch R, Spiegel J, Marsico G, Tannahill D, Balasubramanian S (2018) Genome-wide mapping of endogenous G-quadruplex DNA structures by chromatin immunoprecipitation and high-throughput sequencing. *Nat Protoc* 13:551–564.
- Henderson E, Hardin CC, Walk SK, Tinoco I, Blackburn EH (1987) Telomeric DNA oligonucleotides form novel intramolecular structures containing guanine-guanine base pairs. *Cell* 51:899–908.
- Kaczmarczyk L, Bansal V, Rajput A, Rahman R, Krzyżak W, Degen J, Poll S, Fuhrmann M, Bonn S (2019) Tagger—a Swiss army knife for multiomics to dissect cell type-specific mechanisms of gene expression in mice. *PLoS Biol* 17:e3000374.
- Kang S-G, Henderson E (2002) Identification of non-telomeric G4-DNA binding proteins in human, *E. coli*, yeast, and *Arabidopsis*. *Mol Cells* 14:404–410.
- Kim N (2017) The interplay between G-quadruplex and transcription. *Curr Med Chem* 26:2898–2917.
- Lejault P, Moruno-Manchon JF, Vemu SM, Honarpisheh P, Zhu L, Kim N, Urayama A, Monchaud D, McCullough LD (2020) Regulation of autophagy by DNA G-quadruplexes. *Autophagy* 16:2252–2259.
- Lepack AE, et al. (2020) Dopaminylation of histone H3 in ventral tegmental area regulates cocaine seeking. *Science* 368:197–201.
- Li X, et al. (2019) The DNA modification N6-methyl-2'-deoxyadenosine (m6dA) drives activity-induced gene expression and is required for fear extinction. *Nat Neurosci* 22:534–544.
- Li X, Wei W, Zhao Q-Y, Widagdo J, Baker-Andresen D, Flavell CR, D'Alessio A, Zhang Y, Bredy TW (2014) Neocortical Tet3-mediated accumulation of 5-hydroxymethylcytosine promotes rapid behavioral adaptation. *Proc Natl Acad Sci* 111:7120–7125.
- Marshall PR, et al. (2020) Dynamic regulation of Z-DNA in the mouse prefrontal cortex by the RNA-editing enzyme Adar1 is required for fear extinction. *Nat Neurosci* 23:718–729.
- Marshall P, Bredy TW (2016) Cognitive neuroepigenetics: the next evolution in our understanding of the molecular mechanisms underlying learning and memory? *NPJ Sci Learn* 1:16014.
- Martin SJ, Grimwood PD, Morris RGM (2000) Synaptic plasticity and memory: an evaluation of the hypothesis. *Annu Rev Neurosci* 23:649–711.
- Moruno-Manchon JF, et al. (2020) Small-molecule G-quadruplex stabilizers reveal a novel pathway of autophagy regulation in neurons. *Elife* 11:e52283.
- Nojima T, Gomes T, Carmo-Fonseca M, Proudfoot NJ (2016) Mammalian NET-seq analysis defines nascent RNA profiles and associated RNA processing genome-wide. *Nat Protoc* 11:413–428.
- O'Neill LP, VerMilyea MD, Turner BM (2006) Epigenetic characterization of the early embryo with a chromatin immunoprecipitation protocol applicable to small cell populations. *Nat Genet* 38:835–841.
- Qiao Q, Wang L, Meng FL, Hwang JK, Alt FW, Wu H (2017) AID recognizes structured DNA for class switch recombination. *Mol Cell* 67:361–373.e4.
- Robinson J, Raguseo F, Nuccio SP, Liano D, Di Antonio M (2021) DNA G-quadruplex structures: more than simple roadblocks to transcription? *Nucleic Acids Res* 49:8419–8431.
- Sen D, Gilbert W (1990) A sodium-potassium switch in the formation of four-stranded G4-DNA. *Nature* 344:410–414.
- Vanyushin BF (2006) Enzymatic DNA methylation is an epigenetic control for genetic functions of the cell. *Biochemistry (Mosc)* 70:488–499.
- Vecsey CG, et al. (2007) Histone deacetylase inhibitors enhance memory and synaptic plasticity via CREB: CBP-dependent transcriptional activation. *J Neurosci* 27:6128–6140.
- Wei W, et al. (2012) P300/CBP-associated factor selectively regulates the extinction of conditioned fear. *J Neurosci* 32:11930–11941.
- Zhang X, Spiegel J, Martínez Cuesta S, Adhikari S, Balasubramanian S (2021) Chemical profiling of DNA G-quadruplex-interacting proteins in live cells. *Nat Chem* 13:626–633.